MODELING AND OPTIMIZATION OF SYSTEMS FOR NUTRIENT RECOVERY FROM LIVESTOCK WASTE

EDGAR MARTÍN HERNÁNDEZ

A dissertation submitted for the degree of

DOCTOR IN CHEMICAL SCIENCE AND TECHNOLOGY

at the

UNIVERSIDAD DE SALAMANCA

VNiVERSiDAD D SALAMANCA

CAMPUS OF INTERNATIONAL EXCELLENCE

Academic advisor: Mariano Martín Martín

Programa de Doctorado en Ciencia y Teconología Química

Departamento de Ingeniería Química y Textil

Universidad de Salamanca

February 2022

VNiVERSiDAD D SALAMANCA
CAMPUS OF INTERNATIONAL EXCELLENCE

El **Dr. D. Mariano Martín Martín**, Profesor Titular de Universidad del Departamento de Ingeniería Química y Textil de la Universidad de Salamanca

Informa:

Que la memoria titulada: "Modeling and optimization of systems for nutrient recovery from livestock waste", que para optar al Grado de Doctor en Ciencia y Tecnología Química con Mención Internacional presenta **D. Edgar Martín Hernández**, ha sido realizada bajo nuestra dirección dentro del Programa de Doctorado Ciencia y Tecnología Químicas (RD 99/2011) de la Universidad de Salamanca, y que considerando que constituye un trabajo de tesis.

Autoriza:

Su presentación ante la Escuela de Doctorado de la Universidad de Salamanca, mediante el formato de compendio de publicaciones.

Y para que conste a los efectos oportunos, firmo la presente en Salamanca, a 01 de diciembre de 2021.

Fdo: Mariano Martín Martín

A mi familia, y a todos los que por mi vida pasaron.

Non exiguum temporis habemus, sed multum perdimus.
Satis longa vita et in maximarum rerum consummationem
large data est, si tota bene collocaretur;
sed ubi per luxum ac neglegentiam diffluit,
ubi nulli bonae rei impenditur,
ultima demum necessitate cogente quam ire non
intelleximus transisse sentimus.

— Lucius Annaeus Seneca, De brevitate vitae.

No tenemos un tiempo escaso, sino que perdemos mucho.
La vida es lo bastante larga para realizar las mayores empresas,
pero si se desparrama en la ostentación y la dejadez,
donde no se gasta en nada bueno, cuando al final
nos acosa el inevitable trance final, nos damos cuenta
de que ha pasado una vida que no supimos que estaba pasando.

— Lucius Annaeus Seneca, De la brevedad de la vida.

ACKNOWLEDGMENTS

Complete

ABSTRACT

To be completed.

RESUMEN

Completar.

PUBLICATIONS

This thesis is presented as a compendium of publications, where each of the chapters corresponds to a formal manuscript published in a scientific journal, or currently under review, and book chapters. The relation of manuscripts published or under review, and book chapters that comprise this dissertation is detailed below:

Martín-Hernández, E., Guerras, L., & Martín, M. (2020). Optimal technology selection for the biogas upgrading to biomethane. *Journal of Cleaner Production*, 122032.

Martín-Hernández, E., Hu, Y., Zavala, V., Martín, M., & Ruiz-Mercado, G. (Under Review). Analysis of incentive policies for phosphorus recovery at livestock facilities in the Great Lakes area. *Resources, Conservation & Recycling*.

Martín-Hernández, E., Martín, M., & Ruiz-Mercado, G. (2021). A geospatial environmental and techno-economic framework for sustainable phosphorus management at livestock facilities. *Resources, Conservation & Recycling*, *175*, 105843.

Martín-Hernández, E., Ruiz-Mercado, G., & Martín, M. (2020). Model-driven spatial evaluation of nutrient recovery from livestock leachate for struvite production. *Journal of Environmental Management*, *271*, 110967.

Martín-Hernández, E., Sampat, A., Martin, M., Zavala, V., & Ruiz-Mercado, G. (2021). A Logistics Analysis for Advancing Carbon and Nutrient Recovery from Organic Waste. In *Advances in Carbon Management Technologies* (pp. 186–207). CRC Press.

Martín-Hernández, E., Sampat, A., Zavala, V., & Martín, M. (2018). Optimal integrated facility for waste processing. *Chemical Engineering Research and Design*, *131*, 160–182.

CONTENTS

LIST OF FIGURES

1

INTRODUCTION

1.1 RATIONALE: OVERVIEW OF THE NUTRIENT POLLUTION CHALLENGE

Human population is experiencing a continuous growth since the end of the Black Death in the XIV century (Biraben, 1980), which is at 7.8 billion as of 2020, and it is estimated to be at 9.7 billion and 10.9 billion by 2050 and 2100 respectively (United Nations, Department of Economic and Social Affairs, 2019). Population growth demands increasing amounts of food, which in turn requires an efficient food production system to ensure global food security. In this context, the development of different technical advancements has been a key factor to increase the productivity of the food production system. Notably, crucial developments were achieved in the late modern period[1], including the commercial production of phosphate in 1847 (Samreen & Kausar, 2019), the development of the Haber-Bosch process for the production of synthetic nitrogen-based fertilizers in 1913 (Smil, 1999), and the mechanization of agriculture and the development of the modern intensive farming in the XX century (Constable & Somerville, 2003; Nierenberg & Mastny, 2005).

Despite these advancements have increased the productivity of agriculture and farming industries, multiple environmental impacts associated with them emerges, including water scarcity, greenhouse gases emissions, nutrient pollution of waterbodies, and soil degradation, among others. These threats must be carefully addressed in order to avoid the depletion of natural resources and reach a sustainable food production system.

Focusing on the impacts derived from agriculture and farming on the nutrient cycles, it can be observed that the natural cycles of phosphorus and nitrogen have been altered by these activities (Bouwman, Beusen, & Billen, 2009). Large amounts of nutrients are released into the environment in the form of synthetic fertilizers and livestock manure. Nitrogen and phosphorus are accumulated in soils, creating a nutrient legacy that is further transported to waterbodies by runoff. This process results in the eutrophication of waterbodies, which can lead algal bloom episodes. Algal

1 The terminology used in this dissertation for the periodization of human history follows the English-language historiographical approach. It should be noted that the late modern period is referred to as the contemporary period in the European historiographical approaches.

blooms are events resulting from the rapid increase of algae in a water system which can be promoted by an excess of nutrients in water. These episodes alter the normal functioning of aquatic ecosystems, since they cause hypoxia as a consequence of the aerobic degradation of algal biomass by bacteria. Moreover, some species of algae that cause algal blooms can releases toxins into the water systems. The main flows of nutrient releases into the environment by anthropogenic activities is shown in Figure 1.1.

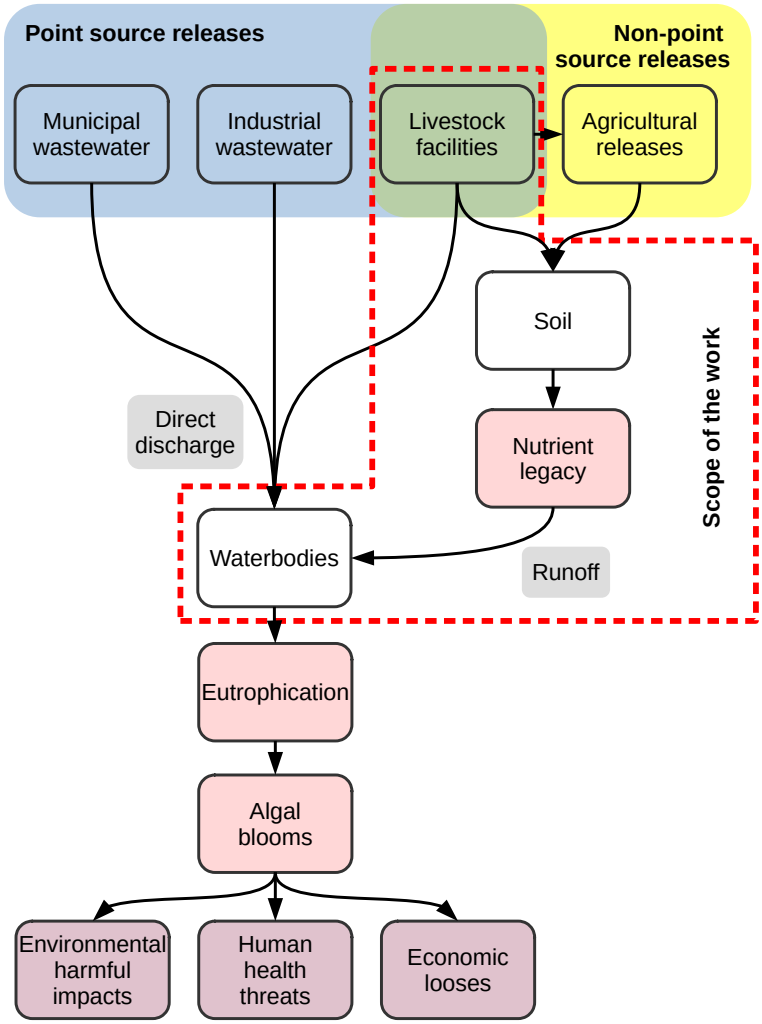

Figure 1.1: Main flows of nutrients released by anthropogenic activities.

In addition to the environmental problems, the use of nutrients for food production also raises geopolitical concerns since phosphorus is one to the most sensitive elements to depletion. Phosphorus is a non-renewable material whose reserves are expeted to be depleted in the next 50 to 100 years. Moreover, no substitute material is currently known (Cordell,

Drangert, & White, 2009). Conversely, synthetic nitrogen can be produced using the atmospheric N_2 as raw material through the Haber-Bosh process. However, nowadays this process relies on non-renewable energy sources, and therefore the production of synthetic nitrogen–based fertilizers is dependent on non-renewable resources as well.

Considering the two challenges described, i.e., nutrient pollution of waterbodies as a consequence of agricultural and farming activities, and the current dependency on non-renewable resources for the production of synthetic fertilizers, nutrient recovery and recycling is not only a desirable but also a necessary approach to develop a sustainable agricultural paradigm and ensure the global food security.

Attending to the nutrient releases from intensive livestock farming facilities, known as concentrated animal feeding operations (CAFOs)[2], several manure management techniques are currently used. The land application of manure is a common technique that allows the recycling of nutrients as fertilizers for crops (Kellogg, Lander, Moffitt, & Gollehon, 2000). However, the increase of intensive livestock farming generates vast amounts of waste generated by CAFOs, e.g., each adult cow generates between 28 and 39 kg of manure per day, and each adult pig generates around 11.5 kg of manure per day (USDA, 2009). Manure processing is commonly based on the separation of liquid and solid phases. The liquid phase can be treated in anaerobic and/or aerobic lagoons for organic matter and pathogens removal, as well as odor control (Tilley, Ulrich, Lüthi, Reymond, & Zurbrügg, 2014). The obtained liquid effluent can be used for irrigation and nutrient supplementation of crops. The solid phase can be composted for the degradation of organic matter and pathogens removal, resulting in a solid material called compost with a larger amount of nitrogen and phosphorus available for plants, which is result of the mineralization of nutrients previously contained in organic compounds. Since compost is also a good source of organic matter for crops, it is a valuable material suitable for sale (Tilley et al., 2014). However, both materials, the liquid effluent obtained from the lagoons and compost, are too bulky to be economically transported to nutrient deficient locations (Burns & Moody, 2002). As a result, livestock waste is usually spread in the surroundings of livestock facilities, at a detrimental cost of environment. This result in the gradual build-up of nutrients in soils, which might lead the harmful environmental impacts previously described.

A promising alternative for abating nutrient releases and reducing the environmental footprint of livestock industry is the implementation of

2 CAFO is a regulatory term defined by the U.S. Environmental Protection Agency for large facilities where animals are kept and raised in confined situations (USDA, 2011). This term is used in this dissertation to denote the intensive livestock farming facilities studied.

processes for the recovery of phosphorus and nitrogen at CAFOs. At the time, that valuable nutrient-rich materials are obtained for the redistribution of phosphorus and nitrogen to nutrient-deficient areas. There exist a number of processes for nutrient recovery from livestock waste, which can be differentiated into those technologies oriented to phosphorus recovery, including struvite precipitation, calcium-based precipitates production, coagulation-flocculation, electrochemical processes, and systems based on solid-liquid separation; and processes focused on nitrogen recovery, such as stripping, membrane separation, waste drying coupled with ammonia scrubbing, and solid-liquid separation processes. We note that anaerobic digestion is an additional process that can be integrated for manure treatment if the generation of biomethane is pursued, and for increasing the amount of recoverable nutrients through the partial mineralization of nutrients contained in organic compounds. It must be noted that only phosphorus and nitrogen in inorganic compounds can be taken by plants, and therefore the recovery of inorganic nutrients will be the target of the processes studied in this thesis.

The multiple processes for the recovery of phosphorus and nitrogen from livestock waste differ in aspects such as recovery efficiency, processing capacity, capital and operating costs, and products obtained. Therefore, a detailed analysis of each CAFO must be performed in order to select the optimal nutrient recovery system attending to type factors such as the type and amount of waste to be processed, the environmental vulnerability to eutrophication of each region, the current or potential installation of anaerobic digestion systems, etc. Additionally, in the decision-making process these factors have to be prioritized, i.e., sorted by relevance, to select the most suitable nutrient recovery system for each particular facility. As example, more economical processes for nutrient recovery, whose recovery efficiencies are typically lower, could be installed in regions with a low risk of eutrophication. Conversely, regions at severe eutrophication risk require highly efficient nutrient recovery systems that may incur in larger investment and operating expenses. In order to perform a systematic evaluation of CAFOs and their context, we introduce a multi-criteria decision analysis (MCDA) framework integrating geospatial environmental data on eutrophication risk at the subbasin level and techno-economic information of the studied processes.

Attending to the regulatory aspect, nowadays most of the efforts for abating of nutrient releases into the environment and mitigating the eutrophication of waterbodies are focused on the limitation of fertilizer application in croplands. The application of fertilizer and manure for nitrogen supplementation in the European Union (EU) is currently regulated by the Nitrates Directive (91/676/EEC) (Grizzetti et al., 2021). Regarding the limitations

for phosphorus application, these are defined at national level. Several European countries have implemented phosphorus application standards based on the different crops and materials used as fertilizers, being generally more restrictive in Northwestern Europe (Amery & Schoumans, 2014).

In sum, it can be observed that nutrient application is limited either in the form of synthetic fertilizers or manure application. However, at present there is a lack of regulation regarding livestock waste treatment (Piot-Lepetit, 2011). In this regard, new efforts to promote the production and adoption of bio-fertilizers obtained from organic waste are being performed through the development of the "Integrated Nutrient Management Plan" (INMAP), which is part of the EU Farm-to-Fork strategy and part of the Circular Economy Action Plan. INMAP should propose actions to promote the recovery and recycling of nutrients, as well as the development of markets for recovered nutrients (ESSP, 2021; Comission, 2020). In this regard, a new regulation for fertilizer products has been released in 2019 (EU 2019/1009), moving struvite and other biofertilizers from the category of waste to fertilizers, establishing a regulatory framework for their use and trade.

In the United States, CAFOs are regulated under the Clean Water Act as point source waste discharges. This regulation sets the need of permits for discharging pollutants to water, which are called National Pollutant Discharge Elimination System (NPDES) permits, including nitrogen and phosphorus releases. These permits must include the necessary provisions for avoiding the harmful effects of the discharges on water and human health (US EPA, 2020b). The development and implementation of a Nutrient Management Plan (NMP) is a required element to obtain an NPDES permit. This document must identify the management practices to be implemented at each CAFO to protect natural resources from nutrient pollution. Land spreading of manure can also be regulated by the NPDES permits, establishing soil nutrient concentration limits and the yearly schedule for manure application. However, no specific methods or processes for waste treatment are defined under federal regulation (US EPA, 2020a). Regarding the use of the recovered nutrients, products obtained from nutrient recovery processes could be classified as waste ny the Clean Water Act, preventing the application of these materials on croplands (NACWA, 2014). However, the U.S. Environmental Protection Agency (US EPA) determined that, although these products could not be directly applied to land under the current regulation, they can be sold as a commodity to be outside of the Clean Water Act restrictions coverage (CNP, 2021). Moreover, US EPA acknowledges that highly refined and primarily inorganic products (such as struvite) could be outside of the scope of these restrictions (CNP, 2021).

Nevertheless, further regulation is needed for defining the products obtained from nutrient recovery processes and to clearly state the conditions for their use as fertilizers on croplands.

Considering the previously described aspects, we note that the regulation of the products obtained from nutrient recovery systems is not totally developed yet either in the European Union and the United States, although important efforts are being performed in order to set a comprehensive regulatory framework for the recycling of phosphorus and nitrogen. Furthermore, no regulation regarding the implementation of nutrient recovery processes has been developed However, both regions have developed previous programs to study and promote the implementation of other technologies for the treatment of livestock and other organic waste. Particularly, the deployment of anaerobic digestion systems have received a considerable support from governmental agencies, resulting in programs such as AgSTAR in the US (US EPA, 2021), and BiogasAction (European Comission, 2021) and BIOGAS^3 (BIOGAS$_3$ PROJECT, 2021) in Europe, among many others. These programs could be a guideline for the development of nutrient recovery plans at CAFOs. In this regard, we have studied the impact of the implementation of nutrient recovery systems in the economy of CAFOs, either considering the deployment of standalone nutrient recovery processes, or integrated systems combining nutrient recovery with anaerobic digestion for the production of electricity and biomethane. Moreover, incentive policies have been analyzed to minimize the negative impact of nutrient recovery on CAFOs economy using the Great Lakes area as case study. In addition, the fair distribution of monetary resources when limited budget is available has been studied using the Nash allocation scheme.

An overview of the main topics studied in this thesis can be observed in Figure 1.2. This work pretends to analyze strategies for promoting effective nutrient recycling addressing studies on the technical, environmental and economic dimensions involved, pursuing the development of sustainable food production paradigm.

.

1.2 APPROACHES FOR PROCESSES MODELING

Process modeling, defined as the mathematical modeling and simulation of systems, falls under the scope of the Process System Engineering (PSE) discipline. These systems include physical, chemical, and/or biological operations. Process modeling forms the foundation for other activities involved in the scope of PSE, including process design, optimal scheduling

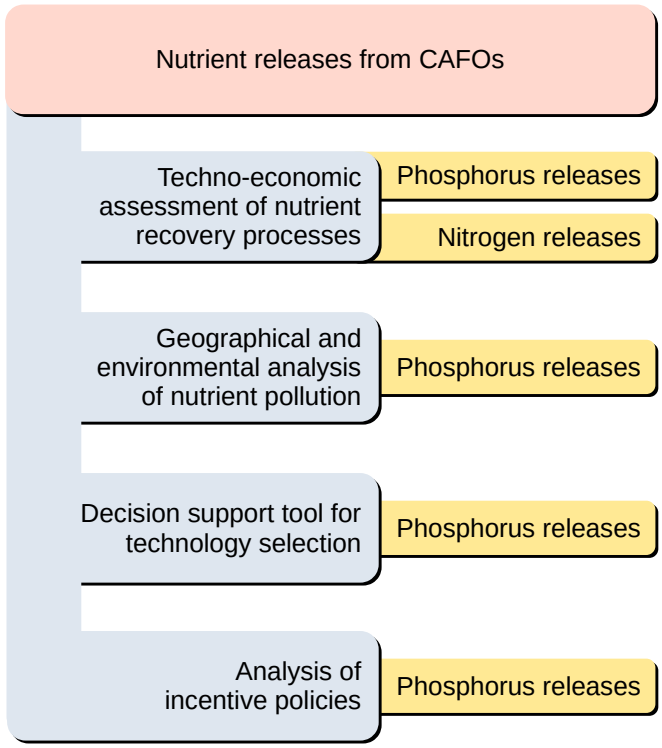

Figure 1.2: Main topics covered in this work.

and planning of the systems operations, and process control (Stephanopoulos & Reklaitis, 2011).

Different modeling techniques have been developed to mathematically describe and represent systems from different domains, including but not limited to the chemical, biochemical, agrochemical, food, and pharmaceutical domains of engineering (Pistikopoulos et al., 2021). An overview of the main modeling techniques is shown in the next sections based on the classification proposed by Martín and Grossmann (2012).

1.2.1 *Short-cut methods*

These type models are the most basic approach to process modeling. They are based on mass, energy, and momentum balances, and can be embedded in other models, such as supply chain models.

1.2.2 *Rules of thumb*

This approach is based on industrial operational data. It provides typical ranges for operating and design values, reflecting the actual parameters of the systems modeled. However, the use of these models is constrained by the availability of data. Compendiums of rules of thumb for different systems can be found in Couper, Penney, Fair, and Walas (2005), Hall (2012), Sadhukhan, Ng, and Hernandez (2014).

1.2.3 *Dimensionless analysis*

This methodology is based on dimensionless groups that describe the performance of a particular system. These models are able to capture the physical meaning of the modeled processes, and they are specially useful to capture scale-up and scale-down issues (Szirtes, 2007).

1.2.4 *Mechanistic models*

This approach relies on first principles for systems modeling, as short-cut models. However, mechanistic models rely in more detailed first principles such as the underlying chemistry, physics or biology that governs the behavior of a particular system. Chemical (Loeppert, Schwab, & Goldberg, 1995) and phase (Brignole & Pereda, 2013) equilibrium models, kinetic models (Buzzi-Ferraris & Manenti, 2009), population balances (Ramkrishna, 2000), and computer fluid dynamics (CFD) (Anderson & Wendt, 1995) fall under this category.

1.2.5 *Surrogate models*

These models aim at developed simplified models from data obtained from rigorous mechanistic models. This approach is widely used for embedding system models into other applications such as process control or supply chain design. Surrogate models building has been systematized into four steps, i.e., design of experiments (DOE), running the rigorous models at the sampling points designated by the DOE, construction of the surrogate model, and validation of the model obtained (Queipo et al., 2005).

Polynomial regression models, in which the relationship between the variables is expressed using a polynomial function, are one of the most basic types of surrogate models. In the case of polynomial regression models involving multiple variables, the optimal variables to be addressed within

the pool of variables considered can be determined by using machine learning-based tools such as ALAMO (Wilson & Sahinidis, 2017), ensuring an optimal trade-off between model accuracy and complexity. Other types of surrogate models are Kriging models, which estimate the relationship between variables as a sum of a linear model and a a stochastic Gaussian function representing the fluctuations of data (Quirante, Javaloyes, & Caballero, 2015), and artificial neural networks (ANN), which are based on generating an input signal as the summation of all the weighted inputs, which is through nodes containing a transfer function. Nodes are connected by edges with assigned weights that adjust the signals transmitted between nodes. Nodes are structured in layers, in a way that nodes receive signals from nodes of the preceding layer, and if the output of the node is above a threshold value defined by the transfer function, sends the output signal to the next layer (Himmelblau, 2000).

1.2.6 *Experimental correlations*

As the surrogate models, experimental correlations are models built using data of the systems represented, but converserly to those one, experimental correlations are built using data from experimental results. Similarly to the rules of thumb, the accuracy of these models is limited by the availability of data, and they are only applicable to the range of operating conditions of the data used for constructing the model.

1.3 APPROACHES FOR DECISION-SUPPORT SYSTEMS

Decision-making activities require to analyze multiple relevant criteria for each course of action. Since criteria often conflict each other, each decision-making process requires the balancing of criteria, prioritizing some criteria over other through the use of some criteria weighting scheme. This procedure requires managing a vast amount of information of conflicting nature, leading to a complex decision-making process. Therefore, different approaches generally called multiple-criteria decision analysis (MCDA) have been developed to explicitly structure and solve decision problems. MDCA aim is to integrate criteria assessment with value judgment to analyze and compare the different available alternatives, identifying the best solution for the specific decision-making context studied. However, it must be highlighted that a certain grade of subjectivity might exist is several steps of MCDA, such as the choice of the set of criteria considered relevant for a particular problem. Therefore, the solution proposed by any MCDA approach must be analyzed considering the assumptions made

for building the problem. In sum, MCDA seeks to structure problems with multiple conflicting criteria, and providing justifiable and explainable solutions to guide decision-makers facing such problems. The solution of a multiple-criteria decision-making problem can be defined as a unique solution representing the most suitable alternative from the set of potential alternatives, or as a subset of satisfactory alternatives (Belton & Stewart, 2002).

An MCDA problem can be articulated in different stages, starting with the problem definition and structuring. At this stage, the goals, constraints, and stakeholders comprising the problem are defined, as well as the different solution alternatives. Based on this information, a model can be built for the assessment and comparison of alternatives. This stage includes the definition of the relevant criteria used for alternatives comparison, their relative priority, and the system for criteria evaluation. Finally, the information retrieved by the model can be used for making informed decisions.

Multi-criteria decision-making problems can be classified into Multi-Attribute Decision Analysis (MADA), which are discrete choice problems where the number of alternatives is finite, and Multi-Objective Decision Analysis (MODA), that are mathematical programming problems that consider infinite number of alternatives, as shown in Figure 1.3. However, we note that mathematical programming techniques are not limited to formulating and solving problems with infinite alternatives, but they can also be used for dealing with discrete decision-making problems (Giove, Brancia, Satterstrom, & Linkov, 2009).

1.3.1 *Multi-Attribute Decision Analysis (MADA)*

In the case of problems consisting of a finite number of alternatives, the suitability of each alternative to the problem given can be measured through its performance according to the multiple criteria considered. A large number of MCDA approaches have been (and are currently being) developed for discrete choice problems, including methods based on value functions (Multi-Attribute Value Theory methods, MAVT) and outranking methods.

1.3.1.1 *Multi-Attribute Value Theory (MAVT)*

INDICATOR-BASED METHODS Multi-Attribute Value Theory (MAVT) approaches are based on an indicator-based methodology for alternatives comparison. The relevant criteria considered in the decision-making process are normalized to a common scale to allow criteria comparison using

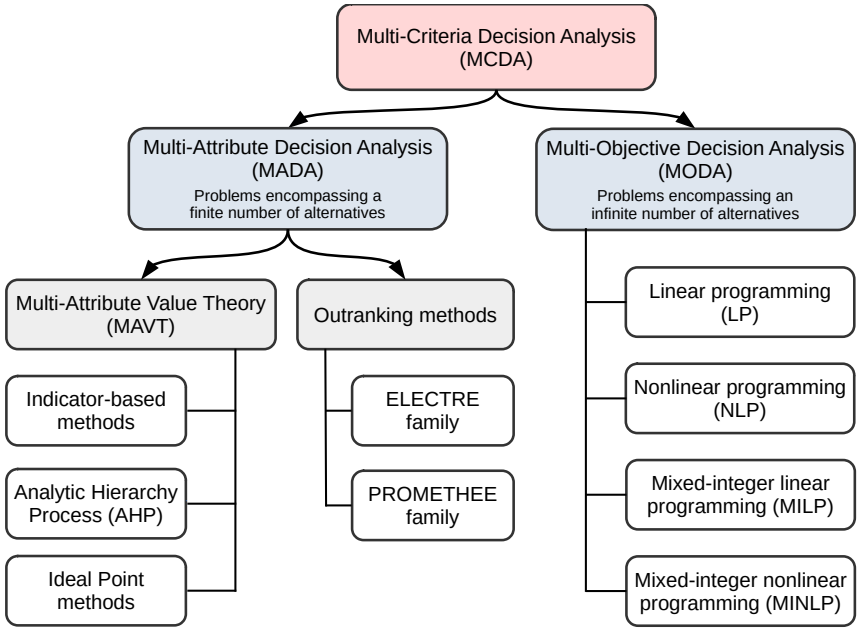

Figure 1.3: Classification of MCDA methods.

an utility or value function. A number of utility functions have been proposed in the literature, including standardization, min-max, and target utility functions (OECD and European Commission, 2008). The normalized criteria are weighted and aggregated to build a composite index, prioritizing some criteria over others. Different aggregation schemes have been proposed, providing different degrees of compensability between indicators, i.e. a deficit in one criteria can be fully, partially, or not compensated by a surplus in other criteria (Gasser et al., 2020). Additive weighting aggregation is a full compensatory method, while geometric and harmonic aggregation methods are partial compensation schemes. Other aggregation schemes include geometric averaging, which is a non-compensatory method, and the Choquet integral (Marichal & Roubens, 2000). The composite index obtained is a single numerical value that can be used to score and rank the proposed alternatives based on their suitability to the criteria considered.

A major source of uncertainty in indicator-based methods is the value of criteria weights. This issue can be addressed using the stochastic multicriteria acceptability analysis (SMAA) method. SMAA is a sensitivity analysis method that address the uncertainty of criteria weights value exploring the feasible space of weights through the Monte Carlo method. Further, details about the SMAA approach can be found in Tervonen and Lahdelma (2007).

In this thesis, and indicator-based methodology has been used to assess and select phosphorus recovery technologies based on technical, environmental, and economic criteria combined in a composite index, as it is shown in Chapter .

ANALYTIC HIERARCHY PROCESS (AHP) Analytic Hierarchy Process (AHP) decomposes the decision problem into multiple simpler sub-problems. These sub-problems are hierarchized and independently analyzed. The sub-problems are solved through the pairwise comparison of alternatives, obtaining numerical indexes that can be used to compare their performance. Finally a numerical weight (priority) is assigned to each element of the hierarchy, and they are used for aggregating the indexes obtained by each alternative at each element of the hierarchy in a final numerical value that can be used to score the overall performance of each alternative accordingly to the set of criteria considered (Saaty, 2000).

IDEAL POINT METHODS Ideal Point methods set an optimal solution, that represent a utopia point where all criteria values are optimal. The performance of each alternative is evaluated through a composite index, that can be constructed using the MAVT approach. The alternatives are ranked based on their relative distance relative to the optimal solution. One of the most common Ideal Point methods is TOPSIS (Hwang & Yoon, 1995).

1.3.1.2 *Outranking methods*

Outranking methods are based on the pairwise comparison of the alternatives for each criterion considered, determining the preferred alternative for each of the criteria. Preference information about all criteria is aggregated to establish evidence for selecting one alternative over another. These methods indicate the dominance of one alternative over another, but they do not quantify the performance gap between the alternatives compared (Giove et al., 2009). Some of the most popular outranking methods are ELECTRE I (Bernard Roy, 1968), II (Bertier Roy & Bertier, 1973), and III (Bernard Roy et al., 1978), and PROMETHEE (Vincke & Brans, 1985).

1.3.1.3 *Multi-Objective Decision Analysis (MODA)*

Problems consisting of an infinite number of solutions require multi-objective mathematical programming (optimization) techniques to be solve. These problems are subjected to a number of equality and/or inequality constraints restricting the solutions that are feasible. The multiple conflicting criteria are combined in an objective function. This objective function

represents the improving level of the criteria, and it will be minimized or maximized for selecting the best solution that represents the optimal trade-off between the different conflicting criteria (Giove et al., 2009). In this thesis, this technique has been employed for determining the operating conditions of processes for the recovery of nutrient, energy and biomethane from livestock waste, as it is shown in Chapters **??** and **??**. Other approach for solving multi-objective mathematical programming problems is to set a priori targets for different criteria, or combinations of criteria, that are considered satisfactory, obtaining the problem solution by minimizing the deviations from these goals. Mathematical programming problems can be also classified according to the use of linear or nonlinear equations, and continuous and/or discrete variables (Giove et al., 2009).

LINEAR PROGRAMMING (LP) Linear programming (LP) refers to those mathematical programming problems based on linear equations and continuous variables. A linear programming problem can be expressed as shown in Eq. 1.1, where x is a vector of dimension n, A is a mxn matrix, c is the n dimension vector of cost coefficients, and the right-hand side b is a vector of dimension m (Grossmann, 2021).

$$\begin{aligned} \min \quad & Z = c^T x \\ \text{s.t.} \quad & Ax \leq b \\ & x \geq 0 \end{aligned} \tag{1.1}$$

The two most widely used methods to solve LP problems are the Simplex algorithm (Murty, 1983) and interior-point methods (Potra & Wright, 2000). The Simplex method is more efficient for solving problems with thousands of variables and constraints, while interior-point is more efficient on very large scale and sparse problems (Grossmann, 2021). These methods are implemented in solvers such as CPLEX (IBM, 2009), Gurobi (Gurobi Optimization, LLC, 2021), or XPRESS (FICO, 2021).

NONLINEAR PROGRAMMING (NLP) Nonlinear programming (NLP) refers to those mathematical programming problems containing nonlinear equations, either in the constrains or in the objective function, and continuous variables. A nonlinear programming problem can be expressed as shown in Eq. 1.2, where x is an n dimension vector, $f(x)$ is the objective function of the problem, $h(x)$ is the set of equality constraints and $g(x)$ is the set of inequality constraints (Floudas, 1995).

$$\begin{aligned} \min \quad & f(x) \\ \text{s.t.} \quad & h(x) = 0 \\ & g(x) \leq 0 \\ & x \in X \subseteq \Re^n \end{aligned} \tag{1.2}$$

Some of the most common algorithms to solve NLP problems are successive quadratic programming (SQP), reduced gradient algorithms, and interior point methods.

SQP algorithms are based on the solution of quadratic programming subproblems. Each subproblem optimizes a quadratic model of the objective function subject to linearized constraints. In each of the iterations a search direction is determined reducing some merit function to ensure problem convergence (Gill, Murray, & Saunders, 2005). SNOPT is a solver based on this method (Gill et al., 2005).

Reduced gradient methods consider a linear approximation of the constraints and eliminate variables to reduce the dimension of the problem. The resulting problem is solved by applying the Newton's method. In each of the iterations, the reduced gradient is calculated, the search direction is determined, and finally a line search is performed minimizing the objective function. MINOS (Murtagh & Saunders, 1983) or CONOPT (Drud, 1985) are solvers based on this algorithm.

Interior point methods reformulate the original NLP problem by means of slack variables to replace the inequalities by equalities and the log-barrier function to handle the non-negativity of the x variables. The new problem is solve applying the Newton's method. IPOPT Wächter and Biegler, 2006 and KNITRO (Waltz & Nocedal, 2004) are solvers based on this approach

MIXED-INTEGER LINEAR PROGRAMMING (MILP) Mixed-integer linear programming (MILP) refers to those mathematical programming problems based on linear equations and containing discrete variables. A mixed-integer linear programming problem can be expressed as shown in Eq. 1.3,where x are continuous variables and y are discrete variables. Typically, discrete variables are binary variables (Grossmann, 2021).

$$\begin{aligned} \min \quad & Z = a^T x + b^T y \\ \text{s.t.} \quad & Ax + By \leq d \qquad (1.3) \\ & x \geq 0 \qquad (1.4) \\ & y \in \{0,1\}^m \end{aligned}$$

A number of methods have been proposed to solve MILP problems, including cutting planes, Benders decomposition, branch and bound search, and branch and cut methods.

Cutting planes consist of a sequence of LP problems in which different cutting planes are generated to cut-off the solution of the relaxed LP. They reduce the feasible region of the linear relaxation of the original problem excluding those solutions that are feasible in the linear relaxation but not in the original MILP problem.

Benders decomposition is based on the generation of a lower and an upper bound of the solution of the MILP problem in each iteration. The upper bound is calculated from the primal problem, which correspond with the original problem where the binary variables have been fixed. Conversely, the lower bound is determined through a master problem, which is a LP problem derived from the original problem by means of the duality theory. Branch and bound method structure the problem in form of a binary tree that includes all possible combinations of binary variables. The tree is explored by solving the relaxed versions of the original problem. If the relaxation does not result in an integer solution (0 or 1), it is necessary to go deeper into the solution tree to explore further combinations of the binary variables. If the result obtained is an integer, the next step is to return to the previous subproblem to explore the alternative branch. However, diverse procedures have been developed to discard certain branches, avoiding the need of exploring the whole tree and reducing the problem (Floudas, 1995).

Branch and cut methods combine branch and bound methods with cutting planes targeting a tighter lower bound. In the different nodes, the relaxed problem is solved. If the solution is not integer, the relaxing problem is solved by adding cutting planes in order to strengthen the lower bound (Grossmann, 2021). Gurobi (Gurobi Optimization, LLC, 2021) and CPLEX (IBM, 2009) are solvers based on this approach.

MIXED-INTEGER NONLINEAR PROGRAMMING (MINLP) Mixed-integer nonlinear programming (MINLP) refers to those mathematical programming problems containing nonlinear equations and discrete variables, typically, binary variables. A mixed-integer nonlinear programming problem can be expressed as shown in Eq 1.5, where x represents a vector of continuous variables, y is the vector of binary variables, $h(x,y)$ and $g(x,y)$ denote the equality and inequality constraints respectively. $f(x)$ represents the objective function (Grossmann, 2021).

$$\begin{aligned} \min \quad & f(x,y) \\ \text{s.t.} \quad & h(x,y) = 0 \\ & g(x,y) \leq 0 \\ & x \in X \subseteq \Re^n \\ & y \in \{0,1\}^m \end{aligned} \tag{1.5}$$

Some algorithms for solving MINLP problems are the generalized Benders decomposition, outer approximation, and generalized cross decomposition.

Generalized Benders decomposition (GBD) is based on the generation of a lower and an upper bound of the solution of the MINLP problem in each iteration. Similarly to the Benders decomposition, the upper bound is calculated from the primal problem, which correspond with the original problem where the binary variables have been fixed. The lower bound is determined through a master problem, which is a LP problem derivated from the original problem by means of the duality theory. In addition, the master problem provides information about the binary variables to be fixed in the next iteration (Floudas, 1995).

Outer approximation (OA) provides a lower and an upper bound in each iteration. As the previous case, the upper bound is calculated from the primal problem. The lower bound is calculate from a master problem obtained based on an outer approximation, i.e., the nonlinear objective function and the constraints are linearized around the primal solution. Additionally, the master problem provides information about the binary variables to be fixed in the next iteration.

Generalized cross decomposition (GCD) is based on the generation of a primal problem that provides an upper bound of the solution and also the Lagrange multipliers for the dual subproblem. The dual problem is used to determine the lower bound of the problem, and provides a vector of binary variables to be fixed in the primal problem. The solution of the primal and dual problems go through convergence tests. If any of these test fails, a master problem is solved. This approach seeks to minimize the number of master problems to be solved since the computational requirements of the this problem are higher. This procedure is repeated at each iteration of the algorithm (Floudas, 1995).

1.4 APPROACHES FOR GEOSPATIAL ENVIRONMENTAL ASSESSMENT

The development of mitigation measures to reduce the environmental footprint of anthropogenic activities requires the previous understanding

and quantification of the environmental impacts associated to each sector. This process, called environmental impact assessment (EIA), involves the analysis of multi-disciplinary information, including environmental, physical, geological, ecological, economic, and social data (Gharehbaghi & Scott-Young, 2018). Since EIA aims to evaluate the environmental impact of an activity on a particular geographical location, all these data have a common geographic component, becoming geospatial data.

Geospatial data can be managed and analyzed through specific systems denoted as geographic information system (GIS). GIS is a key tool for EIA that uses the geographic component of geospatial data as an integrative framework that provides the ability to analyze and map the descriptive information of the locations studied. The geographic component of data is the key element of GIS systems, since the spatial (or spatio-temporal) location is used as a key to relate other descriptive information. From the perspective of EIA, this information can be analyzed, interpreted, and mapped in order to determine the vulnerability level to a particular environmental threat at each location, find relationships between human activities and environmental damages, measure the performance of mitigation and remediation processes, etc.

As a result, the combination of GIS, EIA, and methods for the analysis of multi-dimensional information, such as MCDA, provides tools for the development of strategies to promote the transition to a sustainable paradigm for human growth. In this regard, the development of a sustainable, reliable, and resilient water, energy and food nexus is a major issue for food security and environmental protection.

1.5 THESIS OUTLINE

This dissertation is structured in three parts. Part I is devoted to the study of phosphorus management and recovery, Part II addresses a techno-economic assessment of the technologies for nitrogen recovery, and Part III conducts a techno-economic analysis for determining the optimal biomethane production process in order to integrate biogas production and nutrient recovery processes.

1.5.1 *Part I - Phosphorus management and recovery*

CHAPTER **??** - TECHNOLOGIES FOR PHOSPHORUS RECOVERY. This chapter performs a review of the main processes for phosphorus recovery from livestock waste, identifying the most promising processes to be deployed at CAFOs using a mixed-integer nonlinear programming model.

CHAPTER ?? - ASSESSMENT OF PHOSPHORUS RECOVERY THROUGH STRUVITE PRECIPITATION. This chapter studies the mitigation of phosphorus releases through the deployment of struvite precipitation systems in the watersheds of the contiguous Unites States. Specific surrogate models to predict the production of struvite and calcium precipitates from cattle leachate were developed based on a detailed thermodynamic model. In addition, the variability in the organic waste composition is captured through a probability framework based on the Monte Carlo method.

CHAPTER 1.3.1.1 - GEOSPATIAL ENVIRONMENTAL AND TECHNO-ECONOMIC FRAMEWORK FOR SUSTAINABLE PHOSPHORUS MANAGEMENT AT LIVESTOCK FACILITIES. This chapter presents a decision support framework, COW2NUTRIENT (Cattle Organic Waste to NUTRIent and ENergy Technologies), for the assessment and selection of phosphorus recovery technologies at CAFOs based on environmental information on nutrient pollution and techno-economic criteria. This framework combines eutrophication risk data at subbasin level and the techno-economic assessment of six state-of-the-art phosphorus recovery processes in a multi-criteria decision analysis (MCDA) model. We aimed to provide a useful framework for the selection of the most suitable P recovery system for each particular CAFO, and for designing and evaluating effective GIS-based incentives and regulatory policies to control and mitigate nutrient pollution of waterbodies.

CHAPTER ?? - ANALYSIS OF INCENTIVE POLICIES FOR PHOSPHORUS RECOVERY. This chapter conduct a research on the design and analysis of incentive policies using the COW2NUTRIENT framework for the implementation of phosphorus recovery technologies at CAFOs minimizing the negative impact in the economic performance of CAFOs. Moreover, the fair allocation of monetary resources when the available budget is limited is studied using the Nash allocation scheme.

1.5.2 *Part II - Nitrogen management and recovery*

CHAPTER 3 - MULTI-SCALE TECHNO-ECONOMIC ASSESSMENT OF NITROGEN RECOVERY SYSTEMS FOR SWINE OPERATIONS. This chapter evaluates the main processes for nitrogen recovery at intensive swine operations. A multi-scale techno-economic analysis is performed to estimate the capital and operating costs for different treatment capacities, identifying the most promising processes.

1.5.3 *Part III - Nitrogen management and recovery*

CHAPTER ?? - OPTIMAL TECHNOLOGY SELECTION FOR THE BIOGAS UPGRADING TO BIOMETHANE. This chapter performs a systematic study of different biogas upgrading to biomethane processes in order to identify the optimal process attending to the particular characteristics of the biogas produced from livestock manure. Food waste and wastewater sludge are also included for comparison. We aimed to determine the optimal biomethane production processes for the potential combination of biomethane production and nutrient recovery processes into an integrated resources recovery facility.

BIBLIOGRAPHY

Amery, F. & Schoumans, O. F. (2014). *Agricultural phosphorus legislation in Europe*. Institute for Agricultural, Fisheries Research (ILVO), and Alterra Wageningen UR.

Anderson, J. D. & Wendt, J. (1995). *Computational fluid dynamics*. Springer.

Belton, V. & Stewart, T. (2002). *Multiple criteria decision analysis: an integrated approach*. Springer Science & Business Media.

BIOGAS3 PROJECT. (2021). BIOGAS3 PROJECT - Sustainable small-scale biogas from agri-food waste for energy self-sufficiency. http://www.biogas3.eu/eng/index.html. [Online; accessed 28-September-2021].

Biraben, J. N. (1980). An essay concerning mankind's demographic evolution. *Journal of Human Evolution*, *9*(8), 655–663.

Bouwman, A. F., Beusen, A. H. W., & Billen, G. (2009). Human alteration of the global nitrogen and phosphorus soil balances for the period 1970–2050. *Global Biogeochemical Cycles*, *23*(4). doi:doi.org/10.1029/2009GB003576

Brignole, E. A. & Pereda, S. (2013). *Phase equilibrium engineering*. Newnes.

Burns, R. T. & Moody, L. B. (2002). Phosphorus recovery from animal manures using optimized struvite precipitation. *Proceedings of Coagulants and Flocculants: Global market and technical opportunities for water treatment chemicals*, 1–4.

Buzzi-Ferraris, G. & Manenti, F. (2009). Kinetic models analysis. *Chemical Engineering Science*, *64*(5), 1061–1074.

CNP. (2021). *Review of Applicability of EPA's Part 503 Biosolids Rule on Phosphorus Minerals recovered at Water Resource Recovery Facilities*. CNP.

Comission, E. (2020). *A new Circular Economy Action for a cleaner and more competitive Europe*. European Comission.

Constable, G. & Somerville, B. (2003). *A century of innovation: Twenty engineering achievements that transformed our lives. Chapter 7, Agricultural mechanization*. Joseph Henry Press.

Cordell, D., Drangert, J.-O., & White, S. (2009). The story of phosphorus: global food security and food for thought. *Global environmental change*, *19*(2), 292–305.

Couper, J. R., Penney, W. R., Fair, J. R., & Walas, S. M. (2005). *Chemical process equipment: selection and design*. Gulf professional publishing.

Drud, A. (1985). CONOPT: A GRG code for large sparse dynamic nonlinear optimization problems. *Mathematical programming*, *31*(2), 153–191.

ESSP. (2021). *ESPP input for the EU's "Integrated Nutrient Management Action Plan" (INMAP)*. European Sustainable Phosphorus Platform.

European Comission. (2021). BiogasAction. https://ec.europa.eu/inea/en/horizon-2020/projects/h2020-energy/biofuels-market-uptake/biogasaction. [Online; accessed 28-September-2021].

FICO. (2021). Xpress-Optimizer Reference manual, 20.0 edition. Retrieved from http://www.fico.com/xpress

Floudas, C. A. (1995). *Nonlinear and mixed-integer optimization: fundamentals and applications*. Oxford University Press.

Gasser, P., Suter, J., Cinelli, M., Spada, M., Burgherr, P., Hirschberg, S., ... Stojadinović., B. (2020). Comprehensive resilience assessment of electricity supply security for 140 countries. *Ecological Indicators*, *109*. doi:10.1016/j.ecolind.2019.105731

Gharehbaghi, K. & Scott-Young, C. (2018). GIS as a vital tool for Environmental Impact Assessment and Mitigation. In *IOP Conference Series: Earth and Environmental Science* (Vol. 127, *1*, p. 012009). IOP Publishing.

Gill, P. E., Murray, W., & Saunders, M. A. (2005). SNOPT: An SQP algorithm for large-scale constrained optimization. *SIAM review*, *47*(1), 99–131.

Giove, S., Brancia, A., Satterstrom, F. K., & Linkov, I. (2009). Decision support systems and environment: Role of MCDA. In *Decision support systems for risk-based management of contaminated sites* (pp. 1–21). Springer.

Grizzetti, B., Vigiak, O., Udias, A., Aloe, A., Zanni, M., Bouraoui, F., ... Bielza, M. (2021). How EU policies could reduce nutrient pollution in European inland and coastal waters. *Global Environmental Change*, *69*, 102281.

Grossmann, I. E. [Ignacio E]. (2021). *Advanced Optimization for Process Systems Engineering*. Cambridge University Press.

Gurobi Optimization, LLC. (2021). Gurobi Optimizer Reference Manual. Retrieved from https://www.gurobi.com

Hall, S. M. (2012). *Rules of thumb for chemical engineers*. Butterworth-Heinemann.

Himmelblau, D. M. (2000). Applications of artificial neural networks in chemical engineering. *Korean journal of chemical engineering*, *17*(4), 373–392.

Hwang, C. & Yoon, K. (1995). Multi attribute decision making–an introduction. Sage University Papers.

IBM. (2009). *V12.1: User's Manual for CPLEX*.

Kellogg, R. L., Lander, C. H., Moffitt, D. C., & Gollehon, N. (2000). *Manure Nutrients Relative to the Capacity of Cropland and Pastureland to Assimilate Nutrients: Spatial and Temporal Trends for the United States*. U.S. Department of Agriculture.

Loeppert, R. H., Schwab, A. P., & Goldberg, S. (1995). *Chemical equilibrium and reaction models*. Soil Science Society of America.

Marichal, J.-L. & Roubens, M. (2000). Determination of weights of interacting criteria from a reference set. *European journal of operational Research*, *124*(3), 641–650.

Martín, M. & Grossmann, I. E. [Ignacio E.]. (2012). BIOpt: A library of models for optimization of biofuel production processes. In I. D. L. Bogle & M. Fairweather (Eds.), *22nd European Symposium on Computer Aided Process Engineering* (Vol. 30, pp. 16–20). Computer Aided Chemical Engineering. Elsevier.

Murtagh, B. A. & Saunders, M. A. (1983). *MINOS 5.0 User's Guide*. Stanford Univ CA Systems Optimization Lab.

Murty, K. G. (1983). *Linear programming*. Springer.

NACWA. (2014). *Issue Outline on Resource Recovery from Wastewater and Coverage of 40 C.F.R. Part 503*. National Association of Clean Water Agencies.

Nierenberg, D. & Mastny, L. (2005). *Happier meals: Rethinking the global meat industry*. Worldwatch Institute.

OECD and European Commission. (2008). *Handbook on Constructing Composite Indicators. Methology and User Guide*. OECD.

Piot-Lepetit, I. (2011). *Agricultural externalities and environmental regulation: The case od manure management and spreading land allocation*. Bentham Science Publishers.

Pistikopoulos, E. N., Barbosa-Povoa, A., Lee, J. H., Misener, R., Mitsos, A., Reklaitis, G. V., … Gani, R. (2021). Process systems engineering – The generation next? *Computers & Chemical Engineering*, *147*, 107252.

Potra, F. A. & Wright, S. J. (2000). Interior-point methods. *Journal of Computational and Applied Mathematics*, *124*(1), 281–302.

Queipo, N. V., Haftka, R. T., Shyy, W., Goel, T., Vaidyanathan, R., & Tucker, P. K. (2005). Surrogate-based analysis and optimization. *Progress in aerospace sciences*, *41*(1), 1–28.

Quirante, N., Javaloyes, J., & Caballero, J. A. (2015). Rigorous design of distillation columns using surrogate models based on K riging interpolation. *AIChE Journal*, *61*(7), 2169–2187.

Ramkrishna, D. (2000). *Population balances: Theory and applications to particulate systems in engineering*. Elsevier.

Roy, B. [Bernard]. (1968). Classement et choix en présence de points de vue multiples. *Revue française d'informatique et de recherche opérationnelle*, *2*(8), 57–75.

Roy, B. [Bernard] et al. (1978). ELECTRE III: Un algorithme de classements fondé sur une représentation floue des préférences en présence de criteres multiples. *Cahiers Centre d'Etudes de Recherche Opeérationnelle*.

Roy, B. [Bertier] & Bertier, P. (1973). La Méthode ELECTRE II: Une application au média-planning.

Saaty, T. L. (2000). *Fundamentals of decision making and priority theory with the analytic hierarchy process*. RWS publications.

Sadhukhan, J., Ng, K. S., & Hernandez, E. M. (2014). *Biorefineries and chemical processes: design, integration and sustainability analysis*. John Wiley & Sons.

Samreen, S. & Kausar, S. (2019). Phosphorus Fertilizer: The Original and Commercial Sources. Phosphorus - Recovery and Recycling. IntechOpen. doi:10.5772/intechopen.82240

Smil, V. (1999). Detonator of the population explosion. *Nature*, *400*(6743), 415–415.

Stephanopoulos, G. & Reklaitis, G. V. (2011). Process systems engineering: From Solvay to modern bio- and nanotechnology.: A history of development, successes and prospects for the future. *Chemical Engineering Science*, *66*(19), 4272–4306.

Szirtes, T. (2007). *Applied dimensional analysis and modeling*. Butterworth-Heinemann.

Tervonen, T. & Lahdelma, R. (2007). Implementing stochastic multicriteria acceptability analysis. *European Journal of Operational Research*, *178*(2), 500–513. doi:10.1016/j.ejor.2005.12.037

Tilley, E., Ulrich, L., Lüthi, C., Reymond, P., & Zurbrügg, C. (2014). *Compendium of sanitation systems and technologies*. Eawag.

United Nations, Department of Economic and Social Affairs. (2019). World Population Prospects 2019. https://population.un.org/wpp/Graphs/Probabilistic/POP/TOT/900. [Online; accessed 22-August-2021].

US EPA. (2020a). *Elements of an NPDES Permit for a CAFO. NPDES Permit Writers' Manual for CAFOs*. U.S. Environmental Protection Agency.

US EPA. (2020b). NPDES Permit Basics. https://www.epa.gov/npdes/npdes-permit-basics. [Online; accessed 24-August-2021].

US EPA. (2021). AgSTAR: Biogas Recovery in the Agriculture Sector. https://www.epa.gov/agstar. [Online; accessed 28-September-2021].

USDA. (2009). *Agricultural Wate Management Field Handbook*. U.S. Department of Agriculture.

USDA. (2011). Animal Feeding Operations (AFO) and Concentrated Animal Feeding Operations (CAFO). https://www.nrcs.usda.gov/wps/portal/nrcs/main/national/plantsanimals/livestock/afo/. [Online; accessed 10-August-2021].

Vincke, J. P. & Brans, P. (1985). A preference ranking organization method. The PROMETHEE method for MCDM. *Management Science*, *31*(6), 647–656.

Wächter, A. & Biegler, L. T. (2006). On the implementation of an interior-point filter line-search algorithm for large-scale nonlinear programming. *Mathematical programming*, *106*(1), 25–57.

Waltz, R. A. & Nocedal, J. (2004). KNITRO 2.0 User's Manual. *Ziena Optimization, Inc.[en ligne] disponible sur http://www. ziena. com (September, 2010)*, *7*, 33–34.

Wilson, Z. T. & Sahinidis, N. V. (2017). The ALAMO approach to machine learning. *Computers & Chemical Engineering*, *106*, 785–795.

2

OBJECTIVE

2.1 SCOPE AND OBJECTIVES OF THE THESIS

2.2 MAIN OBJECTIVE

This thesis seeks to promote the recovery and recycling of nutrients contained in livestock waste by identifying the most appropriate technologies for phosphorus and nitrogen recovery at cattle and swine CAFOs, assessing the potential nutrient releases abatement that could be achieved by the deployment of these systems and analyzing incentive policies for their effective implementation at livestock facilities. Moreover, we introduce a systematic framework for evaluating and selecting the most suitable nutrient recovery system at CAFOs considering geospatial environmental vulnerability to nutrient pollution.

2.3 SPECIFIC OBJECTIVES

OBJECTIVE I: To identify the role of intensive farming activities on nutrient pollution, including the main sources of nutrient releases, as well as potential processes and systems for nutrient recovery.

OBJECTIVE II: To identify environmental indicators for nutrient pollution, and use them to assess the potential for the abatement of phosphorus releases by deploying the processes previously selected at livestock facilities at subbasin spatial resolution.

OBJECTIVE III: To develop a decision-support system for the evaluation and selection of nutrient recovery systems at livestock facilities integrating techno-economic data of the nutrient recovery technologies and environmental vulnerability to nutrient pollution information determined through a tailored geographic information system (GIS) in order to select the most suitable system for each particular livestock facility.

OBJECTIVE IV: To design and analyze potential incentive policies for the deployment of phosphorus recovery technologies at livestock facilities, as well as to study the fair allocation of limited monetary resources.

Part I

PHOSPHORUS MANAGEMENT AND RECOVERY

Part II

NITROGEN MANAGEMENT AND RECOVERY

3

MULTI-SCALE TECHNO-ECONOMIC ASSESSMENT OF NITROGEN RECOVERY SYSTEMS FOR SWINE OPERATIONS

3.1 INTRODUCTION

The agricultural sector has experimented an industrialization process since the XIX century, pursuing the intensification of the agri-products and food production, i.e., increasing the agricultural production per unit of input resources, including land, labor and feed among others (FAO, 2004). During the last decades, the agricultural intensification is driven by a sustained increase in the population, the average income growth in both developed and developing countries, and the trade liberalization and logistics advancements leading the transnational trade of products (Baker & Da Silva, 2014). As a result of this intensification process, the largest quantity and variety of agri-products in the human history is produced and distributed nowadays. However, multiple environmental challenges must be faced as a consequence of the industrialization of the agriculture and farming activities: soil depletion of nutrients and organic matter as consequence of mono-cropping, excessive and inefficient use of synthetic fertilizers to maintain high cropping yields, spatial concentration and inappropriate management of livestock manure, biodiversity loss, etc. Focusing in the context of nutrient management, the use of synthetic fertilizers, and the detachment of arable lands and livestock facilities decoupled the previous link where the organic waste from livestock activities were used as nutrient and organic matter supply for crops (Bouwman, Beusen, & Billen, 2009). This decoupling has created a dependency on mineral (phosphorus) and synthetic (nitrogen) fertilizers, and the adequate management of animal manure has become a serious problem for concentrated animal feeding operations (CAFOs). Therefore, there is disconnection between localized areas with large concentrations of organic waste containing nutrients, such as the intensive livestock facilities, and croplands demanding nitrogen and phosphorus relying in synthetic and mineral fertilizers to keep high yield rates. Due to the sparse location of the facilities and the high density of organic wastes, including manure and digestate, the transportation of these wastes for nutrients redistribution is challenging and expensive (Sampat, Martin-Hernandez, Martín, & Zavala, 2018). Therefore, the implementation of technologies and processes for the recovery of nutrients in a form

suitable for easy transport and use in croplands is of utmost importance, restoring the circularity of agricultural nutrients usage disrupted by industrial practices. However, the selection of the most suitable technology for an individual facility is not a trivial process, but involves multiple dimensions, including the recovery efficiency, the effect of the scale on the economic performance of the process, and the environmental footprint of the different technologies. Some previous works assessing and comparing technologies have been performed, but they do not capture the effect of the economies of scale (Munasinghe-Arachchige & Nirmalakhandan, 2020; De Vrieze et al., 2019), or they are limited to a few number of technologies (Bolzonella, Fatone, Gottardo, & Frison, 2018). Beckinghausen, Odlare, Thorin, and Schwede (2020) reports a lack of techno-economic analyses for nitrogen recovery techniques to identify the most suitable process according to the characteristics of each facility. In addition, the previous studies do not capture the effects of integrating these processes with anaerobic digestion systems for energy recovery.

In this work, six state-of-the-art technologies for nitrogen recovery from livestock waste, i.e., transmembrane chemisorption, ammonia evaporation and scrubbing, striping in packed tower, MAPHEX, and struvite production, are systematically assessed and compared. Each system is evaluated performing a material flow analysis (MFA) of the whole process, from waste collection to the final treatment, and a techno-economic analysis (TEA) capturing the effect of the economies of scale on the cost of nitrogen recovery. The objective is to determine the most adequate technologies to close the nutrients loop from livestock to crops, and the optimal conditions for the implementation of these systems. The processes for livestock waste treatment studied involve all stages from waste collection to the production of the nutrient-rich final product: manure preconditioning, optional biogas production valorization, solid-liquid separation of manure or digestate, and nutrients recovery. The assessment of such technologies is performed through detailed mathematical models of the processes based on first principles and experimental data, resulting in a flexible framework able to analyze different combinations and scales of technologies for the treatment of swine waste. The information obtained from the techno-economic assessment of nitrogen recovery technologies is key for the further development of policies to promote nutrient recovery and to mitigate the environmental footprint of swine farming activities.

3.2 METHODS

3.2.1 *Livestock waste*

Swine manure generated by animals at different life stages have different composition, as well as a different waste generation ratio, i.e., waste mass generated per animal per day. Data reported by the US Department of Agriculture (U.S. Department of Agriculture, 2009, 2000) is used to determine the waste flow and composition as a function of the number of animals in a facility and their type, as listed in Table 3.1. AU denotes animal units, which is defined as 1000 pounds (453.6 kg) of live animal (U.S. Department of Agriculture, 2011).

Table 3.1: Swine waste characterization. Adapted from U.S. Department of Agriculture (2009, 2000).

Components to Finish	Units	Sow Gestating	Sow Lactating	Boar	Piglets Nursery	Piglets Grow
Animals:AU	ratio	2.67	2.67	2.67	9.09	9.09
Weight	kg/d AU	11.34	26.76	8.62	39.92	29.48
Volume	m^3/d AU	0.012	0.027	0.0085	0.040	0.031
Moisture	%wt	90	90	90	90	90
TS	kg/d AU	1.13	2.68	0.86	4.54	2.95
VS	kg/d AU	1.04	2.45	0.77	3.99	2.45
N	kg/d AU	0.073	0.20	0.064	0.42	0.24
P	kg/d AU	0.023	0.059	0.023	0.068	0.041
K	kg/d AU	0.050	0.13	0.041	0.16	0.11
$N_{inorganic}$:N_{total}	ratio	0.61	0.61	0.61	0.61	0.61
$N_{organic}$:N_{total}	ratio	0.39	0.39	0.39	0.39	0.39
$P_{inorganic}$:P_{total}	ratio	0.58	0.58	0.58	0.58	0.58
$P_{organic}$:P_{total}	ratio	0.42	0.42	0.42	0.42	0.42

AU: Animal units.
TS: Total solids.
VS: Volatile solids.
N: Nitrogen.
P: Phosphorus.
K: Potassium.

3.2.2 *Nitrogen management systems assessment framework*

Swine manure processing involves several stages from manure collection to resources recovery, as shown in Figure 3.1. In this section the modeling details of each stage are drawn.

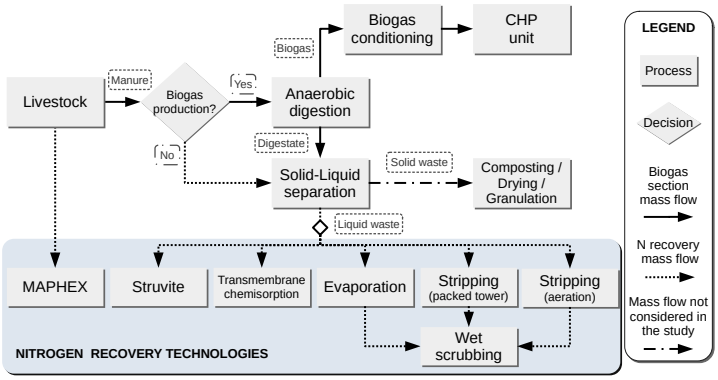

Figure 3.1: Flowchart of the processes assessed for the processing of livestock waste

3.2.2.1 *Anaerobic digestion*

Swine manure can be processed in an anaerobic digestion (AD) unit for the production of biogas and digestate. These materials can be further processed to recover valuable resources, such as electricity and thermal energy from biogas, and nutrients from digestate. As a result of the digestion process, the organic and inorganic fractions of nutrients (i.e., nitrogen and phosphorus) vary due to the partial mineralization of the organic fraction of nitrogen and phosphorus. Therefore, the amount of inorganic nutrients in the digestate is larger than in raw manure, as shown in Table 3.2 (Fangueiro et al., 2020). In addition, the amount of total solids decreases as a consequence of the transformation of volatile solids into biogas. AD process is typically carried out either at mesophilic (25 and 45 °C) and thermophilic (45 and 50 °C) temperatures and atmospheric pressure, with retention times between 30-40 and 15-20 days respectively. There also exist low temperature digestion at psychrophilic conditions ($<$ 25 °C), although it involves longer retention times between 70 and 80 days. The higher the temperature, the shorter the retention time (Al Saedi et al., 2008). A digestion temperature of 40 °C and a retention time (HRT_{AD}) of 21 days have been assumed in this work (Bolzonella et al., 2018).

The composition of biogas produced is based on data reported by Ciborowski (2001). The energy requirements of the AD unit (Q_{digester}), described in Eq 3.1, comprise the energy required for substrate warming up from ambient temperature (assumed to be 12 °C) (Q_{waste}) to the digestion temperature (40 °C), and the energy supplied to offset the digester heat losses (Q_{losses}). The details of the energy balance to the AD unit can be found in the Supplementary Material, Eqs. A.1 to A.8. A maximum di-

Table 3.2: Variation of the inorganic fraction of nutrients biogas generation after anaerobic digestion of swine waste. Adapted from Fangueiro et al. (2020).

Parameter	Variation (%)
TS	-45
VS	-52.5
$N_{inorganic}$	45
$P_{inorganic}$	16

TS: Total solids.
VS: Volatile solids.
N: Nitrogen.
P: Phosphorus .

gester size ($n_{AD,\,max}$) of 6000 m^3 is assumed (Fachagentur Nachwachsende Rohstoffe, 2010).

$$Q_{digester} = Q_{waste} + Q_{losses} \tag{3.1}$$

Correlations for capital expenditures (CAPEX) and operating expenses (OPEX) estimation as a function of animal units have been developed based on data reported by the USDA (Beddoes, Bracmort, Burns, & Lazarus, 2007), as shown in Eqs. 3.2-3.4 and Figure A.1 of the Supplementary Material, where $\dot{m}_{digestate}$ denotes the digestate flow and AU the number of animal units. It should be noted that operating and management (O&M) cost does not include the capital cost amortization.

$$n_{AD} = \left\lceil \frac{\dot{m}_{digestate} \cdot HRT_{AD}}{n_{AD,\,max}} \right\rceil \tag{3.2}$$

$$\text{CAPEX (MM USD (2019))} = \left(2.9069 \cdot 10^{-4} \cdot AU + 0.01625\right) \cdot 1.216 \tag{3.3}$$

$$\text{OPEX} \left(\frac{\text{MM USD (2019)}}{\text{year}}\right) = \left(\frac{15.858 \cdot 10^3}{1 + (AU \cdot 13.917)^{1.461}}\right) \cdot \text{CAPEX} \tag{3.4}$$

3.2.2.2 *Biogas conditioning*

The raw biogas generated is conditioned to remove its impurities. Most of moisture is removed through condensation by compressing and cooling down the biogas stream. H_2S is removed by using a fixed bed of Fe_2O_3, capturing the hydrogen sulfur as Fe_2S_3. The bed can be regenerated using the oxygen contained in air, leading to the formation of elementary sulfur (Ryckebosch, Drouillon, & Vervaeren, 2011). Ammonia and remaining moisture are removed through a pressure swing adsorption (PSA) system. For both processes, two adsorption units are typically installed in-parallel arrangement, so that one unit is in operation while the other bed is undergoing regeneration. Removal yields of 100% have been assumed. More details can be found in Section A.1.2 of the Supplementary Material.

3.2.2.3 *Combined heat and power generation*

Biogas is valorized using a combined heat and power (CHP) unit to produce electricity and heat, which can be used to cover the thermal energy demand of the AD unit, and also for the nitrogen recovery processes if a source of heat is needed, e.g., ammonia evaporation. The energy recovered from biogas is estimated through its low heating value (LHV). LHV of biogas is a function of methane content, and it can be estimated using Eq. 3.5 (Ludington, 2013), where x_{CH_4} refers to the methane mass fraction. Biogas combustion in the CHP unit is performed considering a 20% air excess.

$$LHV_{\text{biogas}}\,(\text{J/m}^3) = -46.26 \cdot 10^6 \cdot x_{CH_4}^2 + 70.87 \cdot 10^6 \cdot x_{CH_4} + 2.29 \cdot 10^6 \tag{3.5}$$

Based on data reported by manufacturers, the electricity and thermal efficiencies assumed are 40% and 50% respectively (Clarke Energy, 2013). The heat produced can be classified in high grade heat (HGH), which is recovered from the exhaust gases of combustion at 450 °C, and low grade heat (LGH) recovered from other points of the equipment at lower temperature. HGH and LGH account for 62% and 38% of total heat energy respectively. LGH is used to cover the energy demand of AD units, while HGH is used for heat-intensive processes such as ammonia evaporation. If LGH from the CHP unit is not enough to cover the energy requirements of AD process, a fraction of HGH can be used to supplement the thermal energy supply.

3.2.2.4 *Digestate solid-liquid separation*

Nutrients contained in manure or digestate form organic and inorganic compounds. On the one hand, organic nutrients are in the form of carbon-based solid compounds, and therefore are mostly contained in the solid phase of waste. The nutrients bonded to organic compounds are not available for plants immediately, but they have to undergo a mineralization process to be transformed into inorganic nutrients (U.S. Department of Agriculture, 2009). On the other hand, inorganic nutrients are those forming inorganic compounds. Since they are water soluble, inorganic nutrients are mostly present in the liquid phase of waste.

The inorganic fraction of nutrients is recovered through a solid-liquid separation stage. The liquid fraction, containing most of inorganic nutrients, will be further processed for nutrient recovery. The solid phase of waste can be composted, promoting the mineralization of a fraction of the organic nutrients. The compost obtained can be used as a nutrient supplementation for crops. A screw press unit is considered for waste liquid-solid phases separation in this study (Møller, Lund, & Sommer, 2000). The partition coefficients for the different components, CAPEX estimation, and electricity consumption considering the discretization of equipment size due to the commercial sizes available, are shown in the Section A.1.3 of the Supplementary Material.

3.2.2.5 *Nitrogen recovery systems*

The technologies for nitrogen recovery assessed in this work, illustrated in Figure 3.2, are described in this section, as well as their main modeling details.

Struvite production (Multiform system): Struvite is a mineral comprised by magnesium, ammonium, and phosphate that can be formed from different organic wastes by the chemical reaction shown in Eq. 3.6. The formation of struvite is a process that can be used for ammonia and phosphorus recovery by precipitation (Edgar Martín-Hernández, Ruiz-Mercado, & Martín, 2020). $MgCl_2$ is supplied to the reactor at a phosphorus to magnesium molar ratio of 2 to increase struvite supersaturation (Bhuiyan, Mavinic, & Koch, 2008). However, since phosphorus concentration in manure is lower than nitrogen concentration, phosphorus acts as the limiting reactant for struvite formation, and in turn, for nitrogen recovery. In this study, pH is adjusted to 9 for optimal struvite formation using sodium hydroxide (Tao, Fattah, & Huchzermeier, 2016).

$$MgNH_4PO_4 \cdot 6H_2O \downarrow \rightleftharpoons Mg^{2+} + NH_4^+ + PO_4^{3-} \tag{3.6}$$

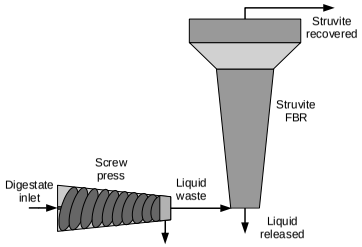

(a) Scheme of MULTIFORM process.

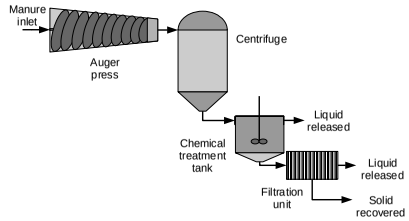

(b) Scheme of MAPHEX process.

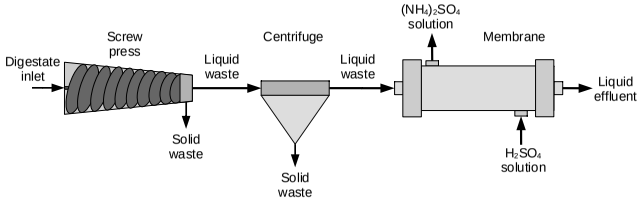

(c) Diagram of a membrane module.

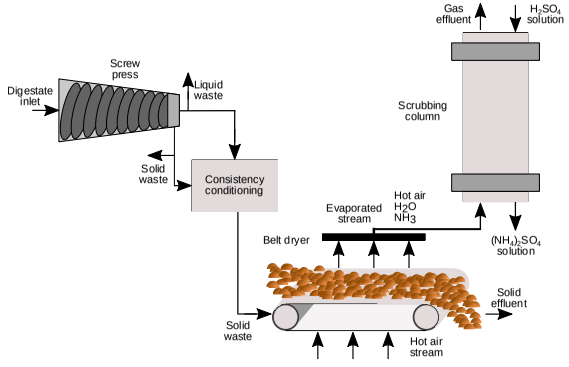

(d) Belt dryer scheme.

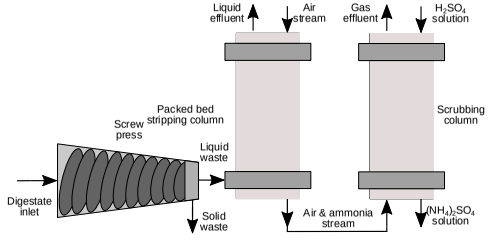

(e) Stripping and scrubber towers scheme.

Figure 3.2: Nitrogen recovery systems assessed in the techno-economic assessment.

Ammonium, phosphate, and other relevant compounds for struvite formation, such as carbonates competing for phosphate ions to form calcium-based precipitates, are part of chemical systems controlled by thermodynamic equilibrium. Therefore, a thermodynamic model for the formation of struvite and calcium precipitates accounting the variability of elements concentration in manure has been developed in a previous work (Edgar Martín-Hernández et al., 2020). The chemical systems considered in the model for estimating struvite formation are included in Tables 1S and 2S of the Supplementary Material. Particularly, we note that calcium ions compete with magnesium ions for the phosphate ions, hindrancing the formation of struvite. Therefore, a correlation to estimate the formation of struvite through the fraction of phosphorus recovered as struvite $\left(x_{\text{struvite}\left(PO_4^{3-}\right)}\right)$ as a function of calcium concentration in the waste has been used in this work, Eq. 3.7 (Edgar Martín-Hernández et al., 2020). $x_{Ca^{2+}:PO_4^{3-}}$ denotes the molar calcium-phosphate ratio, while $\dot{m}_i$ and MW_i refer to the mass flow and molecular weight of the component i respectively. We note that this correlation is valid for estimating struvite formation at a pH of 9. Based on this correlation, the amount of nitrogen recovered is estimated through Eq. 3.9.

$$x_{\text{struvite}\left(PO_4^{3-}\right)} = \frac{0.798}{1 + \left(x_{Ca^{2+}:PO_4^{3-}} \cdot 0.576\right)^{2.113}} \tag{3.7}$$

$$\dot{m}_{\text{struvite } recovered} = \dot{m}_{\text{P } in} \cdot x_{\text{struvite}\left(PO_4^{3-}\right)} \cdot \frac{MW_{\text{struvite}}}{MW_{\text{P}}} \tag{3.8}$$

$$\dot{m}_{\text{N } recovered} = \dot{m}_{\text{struvite } recovered} \cdot \frac{MW_{\text{N}}}{MW_{\text{struvite}}} \tag{3.9}$$

Multiform Harvest is a commercial-level technology selected for the production of struvite from swine waste, since a previous work (Edgar Martín-Hernández, Martín, & Ruiz-Mercado, 2021) found this system as the most cost-effective struvite production process in a wide range of capacities for waste processing. This technology is based on a single pass fluidized bed reactor (FBR), with no recirculation, and conical design, as shown in Fig. 3.2a. The organic waste is pumped to the bottom of the reactor, as well as the magnesium supplement. The struvite particles grow, increasing their size, until their mass overcomes the drag force of the uplift stream. The conical design of the reactor keeps the small and lighter particles on the large diameter section at the top of the reactor, where the superficial velocity is slower. As the particles increase their mass, they settle gradually to lower levels of the reactor, where the diameter is smaller and the superficial velocity and drag force larger, until they are finally

settled on the bottom of the reactor. The liquid phase exits the reactor from the top, where the cross-section is the widest, to ensure the retention of struvite fines.

The techno-economic model for the Multiform process considers a unique size able to process up to 48,000 kg of digestate per day, with an associated capital cost of 625,000 USD per each Multiform unit, plus 420,000 USD for the struvite dryer that serves all Multiform units. The operating cost for the Multiform system unit is 0.012 USD per kg of digestate processed (AMPC, 2018). Revenues by struvite sales of 0.85 USD/kg are also assumed (Molinos-Senante, Hernández-Sancho, Sala-Garrido, & Garrido-Baserba, 2011).

MAPHEX: MAPHEX is a nutrient recovery system based on physico-chemical separations developed by Penn State University and the USDA, Fig. 3.2b. It is conceived as a mobile modular system which can be set in two interconnected truck trailers (C. D. Church, Hristov, Bryant, Kleinman, & Fishel, 2016). MAPHEX involves three stages: liquid-solid separation with a screw press and a centrifuge, addition of iron sulfate to improve nutrients retention, and filtration with diatomaceous earth as filter media. Mass balances for MAPHEX, Eqs. A.15-A.19, are based on experimental data for full-scale modular units reported by Clinton D. Church et al. (2018). The organic solid obtained contains the 93 % of the total solids in the raw waste, with a moisture content of 75%. The 90% of both nitrogen and phosphorus ($\eta^{nutrients}_{\text{MAPHEX}}$) is recovered in this solid material. This combination of processes results in a liquid effluent mostly composed of water with a low content of nutrients, while the nutrients are recovered in a solid stream mainly composed of organic matter. This organic solid has a lower density in nitrogen and phosphorus than other recovered products, such as ammonium sulphate or struvite, resulting in a low market value of this product and hindering the transportation and redistribution of the recovered nitrogen to nutrient-deficient areas.

Each MAPHEX unit is able to process up to 38 ton of manure per day with an associated operation cost of 0.054 USD per kilogram of manure processed. Capital cost of a MAPHEX unit is 291,000 USD (Clinton D. Church et al., 2018; C. D. Church et al., 2016).

Transmembrane chemisorption: Transmembrane chemisorption is a process based on the separation of gaseous species contained in a liquid stream by using a hydrofobic membrane. An acid stripping solution circulates on the lumen side of the membrane to capture the recovered gaseous components. For the case of ammonia recovery, a solution of sulfuric acid is commonly used, resulting in the formation of ammonium sulfate, Eq 3.11. A 10% acid sulfuric solution is considered in this work as stripping fluid (Darestani, Haigh, Couperthwaite, Millar, & Nghiem,

2017). Ammonia recovery efficiency is improved by displacing ammonia-ammonium equilibrium, as shown in Eq. 3.10, to forming of gaseous ammonia raising the pH level up to 11 by adding sodium hydroxide.

$$NH_3 + H^+ \underset{K_a}{\overset{K_b}{\rightleftharpoons}} NH_4^+ \tag{3.10}$$

$$2NH_3 + H_2SO_4 \rightarrow (NH_4)_2\,SO_4 \tag{3.11}$$

Transmembrane chemisorption has been modeled adapting the model proposed by Rongwong and Sairiam (2020), considering mass transfer resistances on digestate liquid, membrane, and permeate phases, species distribution of the ammonia system, and the degree of membrane wetting. Mass transfer resistances on the permeate are considered negligible due to ammonia is rapidly converted into ammonium sulfate as a consequence of the excess concentration of sulfuric acid in this stream.

Membrane size is a function of the digestate flow to be treated. Liquid-Cel™ Extra Flow membranes (3M, 2021) have been considered for ammonia recovery since their use for this purpose has been widely reported in the literature (Darestani et al., 2017; Rongwong & Sairiam, 2020; Linstrom & Mallard, 2001). Membrane characteristics are reported in Table A.7 of the Supplementary Material. Their sizes and costs are collected in Table 3.3. In case the capacity of the largest membrane module is not enough for the treatment of digestate, the installation of several parallel units is considered, as shown in Eq. 3.12. All membrane modules cost have been taken from values reported by manufacturers (SG Projects, 2021; DPC Water Solutions, 2021), except for the Liquid-Cel™ 14x40 module, which price has been estimated based on the cost of the remaining modules, as illustrated in Figure A.3 of the Supplementary Material.

$$n_{\text{parallel}} = \begin{cases} 1 & \text{if } \dot{V}_{\text{digestate}} \leq 125 \frac{\text{m}^3}{\text{h}} \\ \left\lceil \frac{\dot{V}_{\text{digestate}}\left(\frac{\text{m}^3}{h}\right)}{125} \right\rceil & \text{if } \dot{V}_{\text{digestate}} > 125 \frac{\text{m}^3}{\text{h}} \end{cases} \tag{3.12}$$

Membrane sizing is performed through the membrane mass balances, Eqs. A.20-A.53. They are based on the distribution of ammonia species within the digestate, mass transfer on the digestate, wetted membrane, and non-wetted membrane phases, and the diffusion of ammonia through the membrane. Ammonia diffusion through the membrane is driven by bulk and Knudsen diffusivities, which consider the mean free path of molecules and the pore diameter respectively. Therefore, the cross-sectional area of the lumen and shell sides, as well as the lenght of the membrane are

Table 3.3: Liquid-Cel™ membranes size and cost (3M, 2021; SG Projects, 2021; DPC Water Solutions, 2021).

Membrane model	Flow capacity (m3/h)	Diameter (m)	Lenght (m)	Cost (USD)
2.5×8	0.1 - 0.7	0.067	0.200	5,000
4×13	0.5 - 3.4	0.116	0.242	5,700
8x20	1 - 11	0.219	0.406	14,150
10x28	10 - 48	0.279	0.683	17,000
14x40	16 - 125	0.356	1.129	24,300

estimated based on mass balances, as shown in Eqs. A.24, A.25, and A.54 of the Supplementary Material respectively.

One or multiple membrane modules can be needed to achieve the total membrane length (z) needed to reach a certain efficiency, as shown in Eq. 3.13. n_{series} denotes the necessary number of membrane units of length L_{module} in-series arrangement to achieve the desired recovery efficiency. The length of the different membrane units is reported in Table 3.3. n_{parallel} refers to the number of membrane units in-parallel arrangement required to process the waste flow generated at the livestock facility under study based on the processing capacities reported in Table 3.3. Membrane modules CAPEX is estimated through Eq. 3.14, assuming a membrane lifetime (t_{module}) of 10 years (Verrecht, Maere, Nopens, Brepols, & Judd, 2010), and a plant lifetime (t_{plant}) of 20 years. The use of sulfuric acid as stripping fluid and membrane cleaning is the main contributor to membrane OPEX, as shown in Eq. 3.15. Membrane cleaning cost (c_{cleaning}) is reported to be between 2% and 25% of the operating costs (Yu et al., 2020; Verrecht et al., 2010), for which we assume an average value of 13.5%. Additionally, the cost of the pumps needed for driving the digestate and stripping fluid streams through the membrane modules is considered. Cost estimation of pumps is collected in Eqs. A.55 to A.59 of the Supplementary Material.

$$n_{\text{series}} = \left\lceil \frac{z}{L_{\text{module}}} \right\rceil \tag{3.13}$$

$$CAPEX_{\text{membranes}}\,(2019\ \text{USD}) = \left(n_{\text{serie}} \cdot n_{\text{parallel}}\right) \cdot Cost_{\text{module}}\left(\frac{\text{USD}}{\text{module}}\right) \cdot \frac{t_{\text{plant}}}{t_{\text{module}}} \tag{3.14}$$

$$OPEX_{\text{membranes}}\left(\frac{2019\ \text{USD}}{\text{year}}\right) = \frac{\dot{m}_{H_2SO_4}\left(\frac{\text{kg}}{\text{s}}\right)}{\rho_{H_2SO_4}\left(\frac{\text{kg}}{\text{m}^3}\right)} \cdot Price_{H_2SO_4}\left(\frac{\text{USD}}{\text{m}^3}\right) \cdot \frac{1}{1 - \frac{c_{\text{cleaning}}}{100}} \tag{3.15}$$

Total capital and operating expenses for the recovery of nitrogen from livestock digestate using a transmembrane chemisorption process result from the sum of membrane and pump costs are described in Eqs 3.16 and 3.17.

$$CAPEX_{\substack{\text{transmembrane}\\\text{chemisorption}}} = CAPEX_{\text{membranes}} + \sum_{\substack{i\in\\\{\text{shellside,}\\\text{lumenside}\}}} CAPEX_{\text{pumps}_i} \tag{3.16}$$

$$OPEX_{\substack{\text{transmembrane}\\\text{chemisorption}}} = OPEX_{\text{membranes}} + OPEX_{\text{pumps}} \tag{3.17}$$

Ammonia evaporation: Nitrogen can be recovered by ammonia evaporation through digestate drying in a belt dryer unit. The operation of a belt dryer unit requires a minimum concentration of solids of 10% - 12% (Bolzonella et al., 2018). Therefore, the liquid and solid outlet streams from the solid-liquid separation stage are combined to obtain a stream with the desired solids content. After solids content adjustment, digestate is dried in the belt drier, as shown in Fig 3.2d. This unit drys the digestate over the belt with a stream of hot air crossing the belt through orifices on it. Heat (sensible and latent) is transferred from the hot air to the digestate on the belt to increase temperature and evaporate ammonia and a fraction of moisture.

The belt dryer model assumes the evaporation of two components in no equilibrium with a continous extraction of the vapour phase (Treybal, 1980). Since the amount of ammonia in digestate is significantly lower than moisture, air saturation with water vapor is considered the evaporation limit. It must be noted that the moisture carrying capacity of air (i.e., the saturation point) is a function of temperature. This requires to solve the mass and energy balances simultaneously, which are reported in the

Supplementary Material Eqs. shown in Eqs. A.60-A.72. An ammonia removal efficiency $(\eta_{\text{belt dryer}})$ of 80% has been assumed for mass balances calculation (Awiszus, Meissner, Reyer, & Müller, 2018). The assumptions for the modeling of ammonia evaporation by digestate drying are collected in the Section A.1.7 of the Supplementary Material.

Gaseous ammonia is further recovered through acidic scrubbing, as described in Section **??**.

Capital expenses estimation for belt dryer units is based on the energy required for ammonia evaporation. A drying efficiency $(\eta_{\text{belt dryer}})$ of 0.6 has been assumed from the experimental work reported by Sebastian Awiszus, Meissner, Reyer, and Müller (2018). Belt dryer scale-up is based on the correlation proposed by Towler and Sinnott (2012), as shown in Eq. 3.21. The reference values and scale factor used in this correlation are taken from costs and capacities reported by Turley, Hopwood, Burns, and Di Maio (2016), as well as the maximum belt dryer capacity used to compute the number of dryer units needed $(n_{\text{belt dryer}})$, as shown in Eq. 3.19. These data are also used to estimate the scale-up factor, which is estimated equal to 0.7. Belt dryer operating costs are due to electrical consumption, which has been estimated in 0.099 kW of electricity per kW of thermal energy used by the unit, as shown in Eq. 3.22 (Sebastian Awiszus et al., 2018).

$$\dot{Q}^{\text{real}}_{\text{belt dryer}} = \frac{\dot{Q}_{\text{belt dryer}}\,(\text{kW})}{\eta_{\text{belt dryer}}} \tag{3.18}$$

$$n_{\text{belt dryer}} = \left\lceil \frac{\dot{Q}^{\text{real}}_{\text{belt dryer}}\,(\text{kW})}{1000} \right\rceil \tag{3.19}$$

$$\dot{Q}^{\text{design}}_{\text{belt dryer}} = \frac{\dot{Q}^{\text{real}}_{\text{belt dryer}}}{n_{\text{belt dryer}}} \tag{3.20}$$

$$CAPEX_{\text{belt dryer}}\,(2019\ \text{USD}) = \left(n_{\text{belt dryer}} \cdot 214,997 \cdot \left(\frac{\dot{Q}^{\text{design}}_{\text{belt dryer}}\,(\text{kW})}{500} \right)^{0.7} \right) \cdot 1.216 \tag{3.21}$$

$$OPEX_{\text{belt dryer}} \left(\frac{2019\ \text{USD}}{\text{year}} \right) = n_{\text{belt dryer}} \cdot \dot{Q}^{\text{design}}_{\text{belt dryer}}\,(\text{kW}) \cdot 0.099 \left(\frac{\text{kW}_\text{e}}{\text{kW}_\text{t}} \right) \cdot t_{\text{operation}}\,(\text{s}) \cdot 3600 \cdot Price_{\text{electricity}} \left(\frac{\text{USD}}{\text{kWh}} \right) \tag{3.22}$$

Stripping in packed tower: Nitrogen recovery by stripping of the liquid digestate is a widely used technique based on the transfer of ammonia from liquid digestate to an air stream. This operation can be performed either

in packed towers or in bubble column reactors, see Section **??**. Gaseous ammonia is further recovered through acidic scrubbing, as described in Section **??**.

Nitrogen recovery using packed tower stripping, illustrated in Figure 3.2e, has been modeled using the number of transfer units (NTU) method (Metcalf & Eddy, 2014). The pressure drop of tower packing is estimated through the correlation proposed by Kister and Gill (1991), as shown in Eq. 3.23.

$$P\left(\frac{\text{inch water}}{\text{ft}}\right) = 0.115 \cdot \left(F_P\left(\text{ft}^{-1}\right)\right)^{0.7} \tag{3.23}$$

The tower diameter is calculated through the tower flooding capacity. A tower flooding capacity correlation considering the packing pressure drop is developed using ALAMO (Wilson & Sahinidis, 2017) based on the flooding curves developed by Strigle (1994), as shown in Eq. **??** and Figure 3.3. Two-inch (0.051 m) Intalox packing is considered (Strigle, 1994), which packing factor (F_P) is assumed to be 18 ft^{-1} (59 m^{-1}) (Geankoplis, 2003). The operating line considered, defined as the ratio of gas and liquid volumetric flows, can be computed through Eqs. **??** to 3.27, where v_G denotes the superficial gas velocity in $\left(\frac{\text{ft}}{\text{s}}\right)$, ρ_G the gas density in $\left(\frac{\text{lb}}{\text{ft}^3}\right)$, ρ_L the liquid density in $\left(\frac{\text{lb}}{\text{ft}^3}\right)$, ν the kinematic viscosity in (censtokes), $G_G$the gas mass velocity in $\left(\frac{\text{lb}}{\text{ft}^2\cdot\text{s}}\right)$, and G_L the liquid mass velocity in $\left(\frac{\text{lb}}{\text{ft}^2\cdot\text{s}}\right)$ (Strigle, 1994).

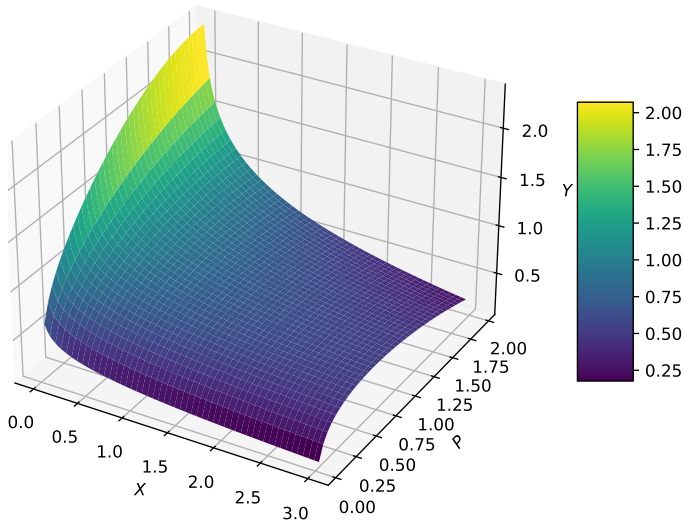

Figure 3.3: Tower flooding capacity correlation considering packing pressure drop.

$$Y = -0.25 \cdot X + 0.22 \cdot \ln(P) - 0.78 \cdot 10^{-1} \cdot P^2 + 0.19 \cdot 10^{-1} \cdot X^3 - 0.39 \cdot X \cdot P + 0.49 \cdot 10^{-2} \cdot (X \cdot P)^3 + 0.89 \tag{3.24}$$

$$Y = v_G \left(\frac{\rho_G}{\rho_L - \rho_G} \right)^{0.5} F_P^{0.5} \nu^{0.05} \tag{3.25}$$

$$X = \log_{10} \left(\frac{G_L}{G_G} \left(\frac{\rho_G}{\rho_L} \right)^{0.5} \right) \tag{3.26}$$

$$\frac{\dot{V}_G}{\dot{V}_L} = 2688 \, \frac{\mathrm{m}^3_{\mathrm{gas}}}{\mathrm{m}^3_{\mathrm{liquid}}} \tag{3.27}$$

$$G_{G_{\mathrm{design}}} = 0.7 G_G = 0.7 \cdot v_G \cdot \rho_G \tag{3.28}$$

The liquid mass velocity is a known parameter since it corresponds to the digestate being processed. The gas velocity is estimated by combining Eqs. 3.23, **??**, and 3.27. The design gas mass velocity considered is 0.7 time the theoretical gas mass velocity, Eq 3.28, while the liquid design mass velocity is computed by combining Eqs. 3.28 and 3.27. Design restrictions reported by Branan (2005) have been considered in the sizing of the packed tower. The tower height is estimated through the height and number of transfer units (Metcalf & Eddy, 2014), as described in the Supplementary Material, Eqs. A.79 to A.84.

The number of stripping units needed $\left(n_{\text{stripping tower}}\right)$ is calculated as the product of the number stripping units in-series arrangement to satisfy the packed towers height limit $\left(n^{\text{series}}_{\text{stripping tower}}\right)$ and the number stripping units in-parallel arrangement to process the amount of waste generated in the livestock facility under evaluation $\left(n^{\text{parallel}}_{\text{stripping tower}}\right)$, as shown in Eq. 3.29. CAPEX of stripping packed towers is estimated based on the columns volume using a correlation based on data from CAPCOST (Turton, 2010), as shown Eq. 3.30. Additionally, capital expenses of compressor units are estimated based on the correlation reported by Almena and Martín (2016), Eq. 3.32. Operating expenses of scrubbing are mainly due to the compression cost, Eq. 3.33.

$$n_{\text{stripping tower}} = n^{\text{series}}_{\text{stripping tower}} \cdot n^{\text{parallel}}_{\text{stripping tower}} \tag{3.29}$$

$$CAPEX_{\text{stripping tower}}\,(2019\ \text{USD}) = 1.216\ n_{\text{stripping tower}} \cdot \left(-6.157 \cdot \left(V_{\text{stripping tower}}\,(\text{m}^3)\right)^2 + 1276.035 \cdot V_{\text{scrubber}}\,(\text{m}^3) + 4007.619\right) \tag{3.30}$$

$$V_{\text{stripping tower}} = \frac{\left(D^{\text{design}}_{\text{stripping tower}}\right)^2 \cdot \pi}{4} \cdot H_{\text{stripping tower}} \tag{3.31}$$

$$CAPEX_{\text{compressor}}\,(2019\ \text{USD}) = 1.216 \cdot \left(335.27 \cdot \dot{W}_{\text{compressor}}\,(\text{kW}) + 36211\right) \tag{3.32}$$

$$OPEX_{\text{compressor}}\left(\frac{2019\ \text{USD}}{\text{year}}\right) = \dot{W}_{\text{compressor}}\,(\text{kW}) \cdot t_{\text{operation}}\,(\text{s}) \cdot 3600 \cdot Price_{\text{electricity}}\left(\frac{\text{USD}}{\text{kWh}}\right) \tag{3.33}$$

Acidic scrubbing: Ammonia contained in the gaseous streams from ammonia evaporation and stripping in packed bed can be recovered in an acidic scrubbing stage using a solution of sulfuric acid in water, as described in Fig. 3.2e. Ammonia is trapped by the liquid stream, reacting with the sulfuric acid to form ammonium sulfate. Mass balances for the scrubber unit consider the water transferred to the gas stream, assuming that saturation is reached, Eq. A.86. Ammonia recovery efficiency ($\eta^{\text{NH}_3}_{scrubber}$) of full-scale ammonia scrubbers has been reported in the range of 40% to 99% (Melse & Ogink, 2005). A typical $\eta^{\text{NH}_3}_{scrubber}$ of 96% has been selected based on the work of Melse and Ogink (2005).

$$\frac{P_{\text{water}}}{Pv_{\text{water}}} = 1 \tag{3.34}$$

$$Pv_{\text{water}} = \frac{\frac{\dot{m}^{\text{gas stream}}_{\text{water}_{out}}}{MW_{\text{water}}}}{\sum_j \frac{\dot{m}^{\text{gas stream}}_j}{MW_j}} \cdot P^{\text{gas stream}}_{in} \tag{3.35}$$

$$\dot{m}^{\text{gas stream}}_{\text{NH}_3\ out} = \dot{m}^{\text{gas stream}}_{\text{NH}_3\ in} \cdot \left(1 - \eta^{\text{NH}_3}_{scrubber}\right) \tag{3.36}$$

The water flow needed to perform the scrubbing operation is computed from the operation line of the unit (L/G), Eq. A.88. Following the rules of thumb for scrubbing units, the design operation line has been assumed as twice the minimum operation line, Eq. A.89. Y_{NH_3} and X_{NH_3} denote the ammonia free basis molar fractions in gas and liquid streams respectively. The amount of sulfuric acid supplied to make-up the sulfate used

for ammonium sulfate formation, Eq. A.91, is slightly larger than the stoichiometric amount of the precipitation reaction, 3.5 $kg_{H_2SO_4}$ per kg_{NH_3} recovered (Bolzonella et al., 2018).

$$(L/G)_{\min} = \frac{Y_{NH_{3in}} - Y_{NH_{3out}}}{X_{NH_{3out}} - X_{NH_{3in}}} \tag{3.37}$$

$$(L/G) = (L/G)_{\min} \cdot 2 \tag{3.38}$$

$$\dot{m}^{\text{liquid stream}}_{\text{water}_{in}} = \left((L/G) \cdot \dot{n}^{\text{liquid stream}}_{\text{total}_{in}} - \dot{n}^{\text{liquid stream}}_{NH_3\ in} \right) \cdot MW_{\text{water}} \tag{3.39}$$

$$\dot{m}^{\text{liquid stream}}_{H_2SO_{4_{in}}} = \dot{m}^{\text{gas stream}}_{NH_3\ in} \cdot \eta^{NH_3}_{scrubber} \cdot 3.5 \tag{3.40}$$

$$\dot{m}^{\text{liquid stream}}_{(NH_4)_2SO_{4_{out}}} = \frac{\dot{m}^{\text{gas stream}}_{NH_3\ in} \cdot \eta^{NH_3}_{scrubber}}{MW_{NH_3}} \cdot MW_{(NH_4)_2SO_{4_{out}}} \tag{3.41}$$

Scrubbing CAPEX is estimated through a preliminary design and sizing of the scrubbing units. As shown in the Section A.1.9 of the Supplementary Material, the estimation of the scrubber diameter is based on the gas velocity in the equipment (Melse & Ogink, 2005). The number of units is set by the maximum diameter of scrubbers, Eq. A.95, which is assumed equal to 1.2 m accordingly to the rules of thumb for packed columns (Branan, 2005). Similarly to the case of stripping columns, the height of scrubbing towers is computed through the transfer units method, as described by Couper, Penney, Fair, and Walas (2005). This method is shown in Eqs. A.96-A.101 of the Supplementary Material.

CAPEX of scrubber units is estimated through the column's volume by using the correlation described in Eq. 3.30. The cost of the compressor is estimated through Eq. 3.32. Operating expenses of scrubbing are mainly related to the use of sulfuric acid, Eq. 3.42, and the compression cost, Eq. 3.43.

$$OPEX_{\text{scrubbers}} \left(\frac{2019\ \text{USD}}{\text{year}} \right) = \frac{\dot{m}_{H_2SO_4} \left(\frac{\text{kg}}{\text{s}} \right)}{\rho_{H_2SO_4} \left(\frac{\text{kg}}{\text{m}^3} \right)} \cdot Price_{H_2SO_4} \left(\frac{\text{USD}}{\text{m}^3} \right) \tag{3.42}$$

$$OPEX_{\text{compressor}} \left(\frac{2019\ \text{USD}}{\text{year}} \right) = \dot{W}_{\text{compressor}}\ (\text{kW}) \cdot t_{\text{operation}}\ (\text{s}) \cdot 3600 \cdot Price_{\text{electricity}} \left(\frac{\text{USD}}{\text{kWh}} \right) \tag{3.43}$$

3.2.3 *Economic assessment*

The total costs of nitrogen recovery and waste processing have been estimated for each nitrogen management system evaluated. These are defined in Eqs. 3.44 and 3.45 respectively for each evaluated technology i, where k represents the possible products obtained, i denotes the discount rate (assumed to be 7%), and n_{plant} represents the process lifetime, which is assumed to be 20 years. Cost estimation includes OPEX and CAPEX amortization of all equipment involved in the processing of swine waste, as well as incomes from the sale of recovered products for those processes producing struvite (Multiform) or ammonium sulphate (digestate drying, stripping in packed tower, and membrane system). The selling prices considered are 0.85 USD per kilogram of struvite (Molinos-Senante et al., 2011), and 0.12 USD per kilogram of ammonium sulphate (Incro, 2021). Conversely, the liquid and organic solid effluents containing low concentrations of nitrogen, such as the products obtained from the MAPHEX system, as well as some streams recovered from other systems such as ammonia evaporation or struvite production, are considered products with no market value. This assumption is based in the fact that, although they can be used for nutrient supplementation in croplands, they are too bulky for being economically transported to nutrient deficient areas. Therefore, similarly to manure, they can just be applied locally, hindering their use as a bio-based substitute of synthetic nitrogen fertilizers.

$$Cost_j^{\substack{nitrogen\\recovery}}\left(\frac{\text{USD}}{\text{kg}_{\text{N recovered}}}\right) = \frac{OPEX_j + CAPEX_j \cdot \frac{i\cdot\left((1+i)^{n_{\text{plant}}}\right)}{\left((1+i)^{n_{\text{plant}}}-1\right)} - \sum_k \dot{m}_{j,k}\cdot Price_k}{\dot{m}_{N_{recovered}}} \tag{3.44}$$

$$Cost_j^{\substack{waste\\processing}}\left(\frac{\text{USD}}{\text{kg}_{\text{Waste processed}}}\right) = \frac{OPEX_j + CAPEX_j \cdot \frac{i\cdot\left((1+i)^{n_{\text{plant}}}\right)}{\left((1+i)^{n_{\text{plant}}}-1\right)} - \sum_k \dot{m}_{j,k}\cdot Price_k}{\dot{m}_{Waste_{processed}}} \tag{3.45}$$

3.3 RESULTS AND DISCUSSION

3.3.1 *Nitrogen flows and recovery efficiency*

The nitrogen flows of the evaluated systems have been analyzed to determine the fraction of nitrogen recovered as inorganic products, either in the form of ammonium sulphate solution or as struvite, the the nitrogen recovered within the organic solid fraction of the waste, and the fraction of nitrogen that it is not recovered and is released into the environment, as shown in Figure 3.4. The nitrogen flows have been analyzed considering the entire recovery systems for waste treatment, including the pretreatment and N recovery processes.

It can be observed that the ammonia evaporation process requires a waste stream with a high solids content for the ammonia evaporation in the belt dryer unit. Therefore, a solid adjustment must be performed, discarding a large fraction of the liquid phase of digestate, which contains most of the inorganic nitrogen. As a result, a significant fraction of nitrogen (79 %) is released in a liquid stream. Nitrogen recovery by stripping in packed tower and membrane systems results in a fraction of nitrogen recovered in the organic solid fraction of the waste as a consequence of liquid-solid separation stages, in addition to the nitrogen recovered as a solution of ammonium sulphate, as illustrated in Figures 3.4d and 3.4e.

Multiform system show a low efficiency of nitrogen recovered as struvite. This is due to the fact that phosphate is the limiting factor for stuvite production, since this compound is in much lower concentrations than nitrogen in swine waste, as reported in Table 3.1. As a result, a significant fraction of nitrogen is not recovered but released in a liquid stream, similarly to ammonia evaporation process, as observed in 3.4b. Finally, since MAPHEX is a manure processing system that integrates all the stages from the feed of raw manure to the recovery of the final products, no pretreatment stages are considered for this system. The nitrogen is recovered within a organic solid material, as shown in Figure 3.4c.

3.3.2 *Economic assessment and scale-up*

The total costs of nitrogen recovery and waste processing for each nitrogen management system evaluated estimated are through Eqs. 3.44 and 3.45, and shown in Figure 3.5. Correlations to estimate the processing cost of the evaluated technologies as a function of animal units are shown in Table 3.4. Significant differences on the processing cost of technologies are observed depending on the reference considered for comparison. Consid-

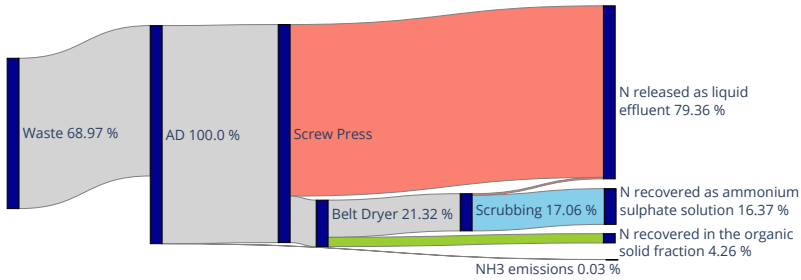

(a) Ammonia evaporation

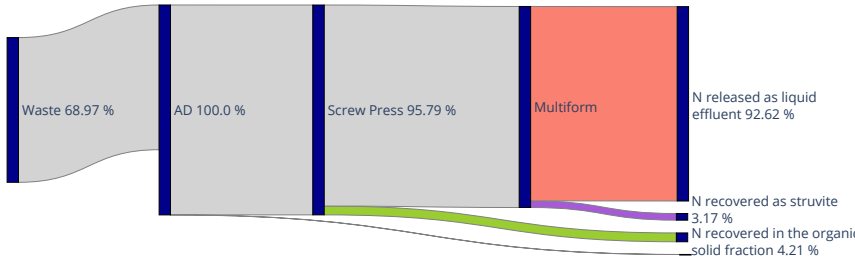

(b) Multiform

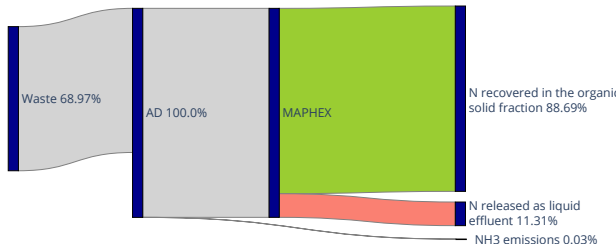

(c) MAPHEX

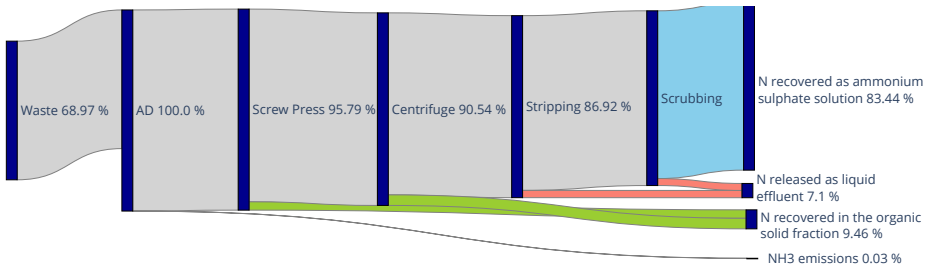

(d) Stripping in packed tower

Figure 3.4: Relative flows of inorganic nitrogen in the studied processes. Since a fraction of organic nitrogen in swine manure is mineralized after the anaerobic digestion of the waste, the 100% refers to the inorganic nitrogen in digestate.

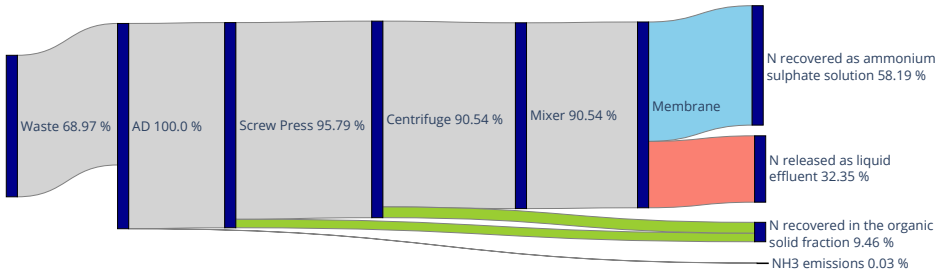

(e) Membrane

Figure 3.4: Relative flows of inorganic nitrogen in the studied processes. Since a fraction of organic nitrogen in swine manure is mineralized after the anaerobic digestion of the waste, the 100% refers to the inorganic nitrogen in digestate.

ering the cost per kilogram of swine waste, illustrated in Figure 3.5a, we observe that Multiform and membrane systems are the processes with the lowest processing cost, 0.13 to 0.02 USD per kg of swine waste processed.

This approach accounts for operating and amortized capital expenses, as well as for the incomes from the sales of recovered products, as shown in Eq. 3.45. This is a common metric used to measure and compare the processing costs of nitrogen recovery processes (De Vrieze et al., 2019; Bolzonella et al., 2018). However, it does not include the nitrogen recovery efficiency of each process, which can lead to the selection of processes with low waste treatment cost, and low nitrogen recovery efficiency. Therefore, we consider that measuring the processing cost as a function of the recovered nitrogen, as shown in Figure 3.5b, is a more accurate metric for comparing different systems. Accordingly to this approach, the economic performance of Multiform dramatically decreases as a result of the low nitrogen recovery efficiency of this technology. Conversely, MAPHEX is revealed as more competitive process when the nitrogen recovered is considered. Since MAPHEX is a single size modular technology, its recovery cost shows a linear behavior, slightly affected by adding extra in-parallel modules to process large amounts of waste. Membrane system is the process with the lowest nitrogen recovery cost, from 10.4 to 3.4 USD per kilogram of nitrogen recovered, depending on the waste processing capacity of the system.

We note that the cost of anaerobic digestion stage represents a large fraction of capital expenses. However, this technology might be already implemented in some swine operations. Therefore, the impact of AD in the CAPEX, OPEX and processing costs has been analyzed. Figures 3.5 and 1S show these costs including AD stages, and Figures 2S and 3S illustrate the

costs of nitrogen recovery systems excluding AD. It can be observed that CAPEX costs are significantly higher when AD is considered. This turns into a decrease of processing costs when AD is not considered. Additional correlations for cost estimation are reported in Table 1S.

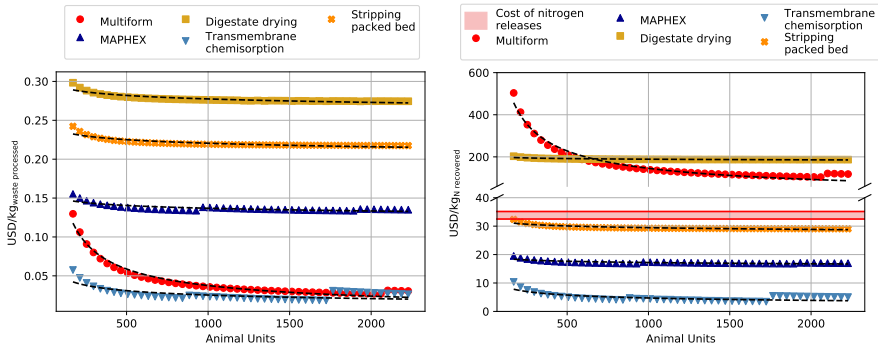

(a) Waste processing cost

(b) Nitrogen recovery cost

Figure 3.5: Processing cost for different livestock facility sizes, including the cost of pretreatment and AD stages.

Additionally, the cost of releasing nitrogen to the environment is illustrated in Figure 3.5b in order to determine the processes for which nitrogen recovery is more economically beneficial than nitrogen release. The releasing cost of nitrogen is estimated based on the environmental and social cost of atmospheric NH_3 releases, and land, freshwater, and groundwater nitrogen loading. The cost of nitrogen release considering these damages reported by Sobota, Compton, McCrackin, and Singh (2015) and Compton, Leach, Castner, and Galloway (2017) are 32.5 and 35.15 USD/$kg_{N\ released}$ respectively. We note that the recovery of nitrogen by using membrane systems, MAPHEX, and stripping in packed tower result in economic savings with respect to nitrogen release to the environment. This information can be a driver for the deployment of swine waste treatment processes for nitrogen recovery. However, a debate can be raised regarding what stakeholders should cover the cost of nitrogen recovery from swine industry. On the one hand, if nitrogen recovery is not performed at swine facilities, nitrogen releases result in environmental remediation costs in the long-term. These costs are usually covered by national and regional governments, which are ultimately funded by taxpayers. As a result, the environmental impact is covered by all citizens, whether or not they benefit from such businesses. On the other hand, the implementation of nutrient recovery systems could impact the economy of swine farms, which in turn could result in the raise of swine products cost, impacting the final consumers. This approach might seem fairer, since it only involves producers and consumers of swine

Table 3.4: Correlations to estimate the processing cost of the evaluated technologies as a function of animal units (AU), including the cost of AD stage.

System	Correlation	Waste processing cost ($USD/kg_{waste\ processed}$) Parameters	Total nitrogen recovery cost ($USD/kg_{N\ recovered}$) Parameters
Ammonia evaporation		a=0.326 b=-0.0233	a=221.805 b=-0.0233
Multiform		a=3.308 b=-0.648	a=12837.477 b=-0.648
MAPHEX	$C = a \cdot AU^b$	a=0.177 b=-0.0372	a=22.240 b=-0.0372
Stripping in packed tower		a=0.271 b=-0.0298	a=36.181 b=-0.0298
Membrane		a=0.188 b=-0.290	a=33.612 b=-0.284

products. However, it would lead to comparative disadvantages between different swine farms as a result of the savings in nitrogen recovery costs due to the economies of scale, as shown in Figure 3.5a. Consequently, small facilities would be more affected by nitrogen recovery than large farms. Therefore, alternative economic schemes should be developed to mitigate the economic impact of the implementation of nitrogen recovery systems at swine facilities. In this regard, previous efforts developed for phosphorus recovery at livestock facilities can be adapted for nitrogen recovery. For instance, the development of a market for trading emissions allowances has been proposed for phosphorus releases from livestock farms (Sampat, Ruiz-Mercado, & Zavala, 2018). This scheme can also be explored for nitrogen releases. Additionally, OJO ACTUALIZAR REFERENCIA!!! E. Martín-Hernández, Hu, Zavala, Martín, and Ruiz-Mercado (Under Review) have studied several incentive policies for the implementation of phosphorus recovery systems in livestock facilities, including the fair allocation of limited incentive budgets, which could be adapted to the case of nitrogen recovery.

3.4 CONCLUSIONS

Intensive swine operations generate vast amounts of organic waste that it is a source of nitrogen releases into the environment. Since these releases are a significant contributor to the eutrophication of waterbodies, and they can result in harmful environmental impacts such as algal bloom episodes, the recovery of nitrogen at livestock facilities is a desirable measure to reduce the environmental footprint of the food production system.

Several processes have been developed for nitrogen recovery from organic waste, and therefore the selection of the most suitable process has to be addressed considering multiple dimensions, including the nitrogen recovery efficiency, the capital and operating expenses, and the impact of the economies of scale in the final cost of nitrogen recovery. A multi-scale techno-economic study has been performed in order to determine the most suitable nitrogen recovery system based on the waste treatment capacity. The mass flows throughout all stages from manure collection to the final treatments have been analyzed in order to determine the nitrogen flows throughout each studied system. Two metrics have been considered to measure the operating cost of each technology, the waste treatment cost ($USD/kg_{\text{waste processed}}$), that it is a metric widely used in literature, and the nitrogen recovery cost ($USD/kg_{\text{N recovered}}$). Since the first metric does not account for the nitrogen recovery efficiency of each system, significant differences on the relative performance among the different technologies are found. This is because some technologies that result in low waste treatment costs show low nitrogen recovery efficiencies, resulting in comparatively large nitrogen recovery costs. However, transmembrane chemisorption is revealed as the most cost-effective nitrogen recovery technology, resulting in costs of 0.02-0.06 $USD/kg_{\text{waste processed}}$, and 3.4-10.4 $USD/kg_{\text{N recovered}}$. Moreover, comparing the negative economic impact of nitrogen releases into the environment, estimated between 32.5 and 35.15 $USD/kg_{\text{N released}}$ with the cost of nitrogen recovery, three technologies reveal to be economically advantageous, transmembrane chemisorption, MAPHEX, and stripping in packed bed.

Future research is needed to discuss what stakeholders in the production and consumption cycle should assume the costs associated with nitrogen recovery. Additionally, further studies have to be addressed to design and evaluate incentive policies for the effective deployment of nitrogen recovery systems at intensive swine operations.

ACKNOWLEDGMENTS

The authors acknowledge funding from the Junta de Castilla y León, Spain, under grant EDU/556/2019.

Disclaimer: The views expressed in this article are those of the authors and do not necessarily reflect the views or policies of the U.S. Environmental Protection Agency. Mention of trade names, products, or services does not convey, and should not be interpreted as conveying, official U.S. EPA approval, endorsement, or recommendation.

BIBLIOGRAPHY

3M. (2021). *3M™Liqui-Cel™Data Sheets*. 3M.

Al Saedi, T., Rutz, D., Prassl, H., Köttner, M., Finsterwalder, T., Volk, S., & Janssen, R. (2008). *Biogas Handbook*. Esbjerg: University of Southern Denmark.

Almena, A. & Martín, M. (2016). Technoeconomic analysis of the production of epichlorohydrin from glycerol. *Industrial & Engineering Chemistry Research*, *55*(12), 3226–3238.

AMPC. (2018). Struvite or Traditional Chemical Phosphorus Precipitation – What Option Rocks? https://www.ampc.com.au/uploads/cgblog/id408/2018-1026_-_Final_Report.pdf. [Online; accessed 20-March-2019].

Awiszus, S., Meissner, K., Reyer, S., & Müller, J. (2018). Ammonia and methane emissions during drying of dewatered biogas digestate in a two-belt conveyor dryer. *Bioresource technology*, *247*, 419–425.

Awiszus, S. [Sebastian], Meissner, K., Reyer, S., & Müller, J. (2018). Utilization of digestate in a convective hot air dryer with integrated nitrogen recovery. *Landtechnik*, *73*(4), 106–114.

Baker, D. & Da Silva, C. (2014). *Trends in agri-food systems: Drivers, changes, impacts and overall assessment*. FAO Policy Learning Programme.

Beckinghausen, A., Odlare, M., Thorin, E., & Schwede, S. (2020). From removal to recovery: An evaluation of nitrogen recovery techniques from wastewater. *Applied Energy*, *263*, 114616.

Beddoes, J. C., Bracmort, K. S., Burns, R. T., & Lazarus, W. F. (2007). *An Analysis of Energy Production Costs from Anaerobic Digestion Systems on U.S. Livestock Production Facilities*. U.S. Department of Agriculture.

Bhuiyan, M., Mavinic, D., & Koch, F. (2008). Phosphorus recovery from wastewater through struvite formation in fluidized bed reactors: a sustainable approach. *Water Science and Technology*, *57*(2), 175–181.

Bolzonella, D., Fatone, F., Gottardo, M., & Frison, N. (2018). Nutrients recovery from anaerobic digestate of agro-waste: Techno-economic assessment of full scale applications. *Journal of environmental management*, *216*, 111–119.

Bouwman, A., Beusen, A. H., & Billen, G. (2009). Human alteration of the global nitrogen and phosphorus soil balances for the period 1970–2050. *Global Biogeochemical Cycles*, *23*(4).

Branan, C. R. (2005). *Rules of Thumb for Chemical Engineers (Fourth Edition)* (Fourth Edition). Burlington: Gulf Professional Publishing. doi:https://doi.org/10.1016/B978-075067856-8/50000-1

Church, C. D. [C. D.], Hristov, A. N., Bryant, R. B., Kleinman, P. J. A., & Fishel, S. K. (2016). A Novel Treatment System to Remove Phosphorus from Liquid Manure. *Appl. Eng. Agric.* *32*(1), 103–112. doi:10.13031/aea.32.10999

Church, C. D. [Clinton D.], Hristov, A. N., Kleinman, P. J., Fishel, S. K., Reiner, M. R., & Bryant, R. B. (2018). Versatility of the MAnure PHosphorus EXtraction (MAPHEX) System in Removing Phosphorus, Odor, Microbes, and Alkalinity from Dairy Manures: A Four-Farm Case Study. *Applied Engineering in Agriculture*, *34*(3), 567–572. doi:10.13031/aea.12632

Ciborowski, P. (2001). *Anaerobic Digestion of Livestock Manure for Pollution Control and Energy Production: A Feasibility Assessment*. Minnesota Pollution Control Agency.

Clarke Energy. (2013). *CHP efficiency for biogas*. Clarke Energy.

Compton, J. E., Leach, A. M., Castner, E. A., & Galloway, J. N. (2017). Assessing the social and environmental costs of institution nitrogen footprints. *Sustainability: The Journal of Record*, *10*(2), 114–122.

Couper, J. R., Penney, W. R., Fair, J. R., & Walas, S. M. (2005). *Chemical process equipment: selection and design*. Gulf Professional Publishing.

Darestani, M., Haigh, V., Couperthwaite, S. J., Millar, G. J., & Nghiem, L. D. (2017). Hollow fibre membrane contactors for ammonia recovery: Current status and future developments. *Journal of environmental chemical engineering*, *5*(2), 1349–1359.

De Vrieze, J., Colica, G., Pintucci, C., Sarli, J., Pedizzi, C., Willeghems, G., … Peng, L., et al. (2019). Resource recovery from pig manure via an integrated approach: A technical and economic assessment for full-scale applications. *Bioresource technology*, *272*, 582–593.

DPC Water Solutions. (2021). *Debubblers*. DPC Water Solutions.

Fachagentur Nachwachsende Rohstoffe. (2010). *Biogas Guide. From production to use.*

Fangueiro, D., Snauwaert, E., Provolo, G., Hidalgo, D., Adani, F., Kabbe, C., … Brandsma, J. (2020). *Mini-paper - Available technologies for nutrients*

recovery from animal manure and digestates. EIP-AGRI Focus Group-Nutrient recycling.

FAO. (2004). *The ethics of sustainable agricultural intensification*. FAO, Rome.

Geankoplis, C. J. (2003). *Transport processes and separation process principles:(includes unit operations)*. Prentice Hall Professional Technical Reference.

Incro. (2021). Ammonium suphate price. Personal communication.

Kister, H. & Gill, D. (1991). Predict flood point and pressure drop for modern random packings. *Chemical engineering progress*, *87*(2), 32–42.

Linstrom, P. J. & Mallard, W. G. (2001). The NIST Chemistry WebBook: A chemical data resource on the internet. *Journal of Chemical & Engineering Data*, *46*(5), 1059–1063.

Ludington, D. (2013). *Calculating the Heating Value of Biogas*. DLtech, Inc.

Martín-Hernández, E. [E.], Hu, Y., Zavala, V., Martín, M., & Ruiz-Mercado, G. (Under Review). Analysis of incentive policies for phosphorus recovery at livestock facilities in the Great Lakes area. *Resources, Conservation & Recycling*.

Martín-Hernández, E. [Edgar], Martín, M., & Ruiz-Mercado, G. J. (2021). A geospatial environmental and techno-economic framework for sustainable phosphorus management at livestock facilities. *Resources, Conservation and Recycling*, *175*, 105843.

Martín-Hernández, E. [Edgar], Ruiz-Mercado, G. J., & Martín, M. (2020). Model-driven spatial evaluation of nutrient recovery from livestock leachate for struvite production. *Journal of Environmental Management*, *271*, 110967.

Melse, R. W. & Ogink, N. (2005). Air scrubbing techniques for ammonia and odor reduction at livestock operations: Review of on-farm research in the Netherlands. *Transactions of the ASAE*, *48*(6), 2303–2313.

Metcalf & Eddy. (2014). *Wastewater Engineering: Treatment and Resource Recovery*. McGraw-Hill, New York.

Molinos-Senante, M., Hernández-Sancho, F., Sala-Garrido, R., & Garrido-Baserba, M. (2011). Economic feasibility study for phosphorus recovery processes. *Ambio*, *40*(4), 408–416.

Møller, H., Lund, I., & Sommer, S. (2000). Solid-liquid separation of livestock slurry: effciency and cost. *Bioresour. Technol. 74*, 223–229.

Munasinghe-Arachchige, S. P. & Nirmalakhandan, N. (2020). Nitrogen-fertilizer recovery from the centrate of anaerobically digested sludge. *Environmental Science & Technology Letters*, *7*(7), 450–459.

Rongwong, W. & Sairiam, S. (2020). A modeling study on the effects of pH and partial wetting on the removal of ammonia nitrogen from wastewater by membrane contactors. *Journal of Environmental Chemical Engineering*, *8*(5), 104240.

Ryckebosch, E., Drouillon, M., & Vervaeren, H. (2011). Techniques for transformation of biogas to biomethane. *Biomass and bioenergy*, *35*(5), 1633–1645.

Sampat, A. M., Martin-Hernandez, E., Martín, M., & Zavala, V. M. (2018). Technologies and logistics for phosphorus recovery from livestock waste. *Clean Technologies and Environmental Policy*, *20*(7), 1563–1579.

Sampat, A. M., Ruiz-Mercado, G. J., & Zavala, V. M. (2018). Economic and environmental analysis for advancing sustainable management of livestock waste: A Wisconsin Case Study. *ACS sustainable chemistry & engineering*, *6*(5), 6018–6031.

SG Projects. (2021). *Gas Transfer Membranes*. SG Projects.

Sobota, D. J., Compton, J. E., McCrackin, M. L., & Singh, S. (2015). Cost of reactive nitrogen release from human activities to the environment in the United States. *Environmental Research Letters*, *10*(2), 025006.

Strigle, R. F. (1994). *Packed tower design and applications: random and structured packings*. Gulf Pub Co.

Tao, W., Fattah, K., & Huchzermeier, M. (2016). Struvite recovery from anaerobically digested dairy manure: A review of application potential and hindrances. *J. Environ. Manage. 169*, 46–57.

Towler, G. & Sinnott, R. (2012). *Chemical engineering design: principles, practice and economics of plant and process design*. Elsevier.

Treybal, R. E. (1980). Mass transfer operations. *New York*, *466*.

Turley, D., Hopwood, L., Burns, C., & Di Maio, D. (2016). *Assessment of Digestate Drying as an Eligible Heat Use in the Renewable Heat Incentive*. NNFCC.

Turton, R. (2010). *CAPCOST software to accompany: Analysis, synthesis, and design of chemical processes*. Upper Saddle River, N.J: Prentice Hall PTR.

U.S. Department of Agriculture. (2000). *Manure Nutrients Relative to the Capacity of Cropland and Pastureland to Assimilate Nutrients*. United States Department of Agriculture.

U.S. Department of Agriculture. (2009). *Waste Management Field Handbook*.

U.S. Department of Agriculture. (2011). Animal Feeding Operations (AFO) and Concentrated Animal Feeding Operations (CAFO). https://www.nrcs.usda.gov/wps/portal/nrcs/main/national/plantsanimals/livestock/afo/. [Online; accessed 10-August-2020].

Verrecht, B., Maere, T., Nopens, I., Brepols, C., & Judd, S. (2010). The cost of a large-scale hollow fibre MBR. *Water Research*, *44*(18), 5274–5283.

Wilson, Z. T. & Sahinidis, N. V. (2017). The ALAMO approach to machine learning. *Computers & Chemical Engineering*, *106*, 785–795.

Yu, H., Li, X., Chang, H., Zhou, Z., Zhang, T., Yang, Y., ... Liang, H. (2020). Performance of hollow fiber ultrafiltration membrane in a full-scale

drinking water treatment plant in China: a systematic evaluation during 7-year operation. *Journal of Membrane Science*, *613*, 118469.

Part III

INTEGRATION OF ANAEROBIC DIGESTION AND NUTRIENT MANAGEMENT SYSTEMS

Part IV

APPENDIX

A

APPENDIX D: SUPPLEMENTARY INFORMATION OF CHAPTER 6

A.1 MODELING DETAILS OF NUTRIENT RECOVERY PROCESSES

A.1.1 *Anaerobic digestion*

The energy requirements of AD unit, described in Eq A.1, comprise the energy required for substrate warming from ambient temperature (considered equal to central Spain average annual temperature, 12 °C) to the digestion temperature (40 °C), Eq. A.2, and the energy supplied to offset the digester heat losses, Eq. A.3. The global heat transfer coefficients (U) for the different digester surfaces are collected in Table A.1. The area of different surfaces is estimated through preliminar equipment design, Eqs. A.4 to A.8, assuming a maximum digester of 6000 m^3 (Fachagentur Nachwachsende Rohstoffe, 2010). The installation of multiple digestion units is considered if the waste flow exceeds this capacity.

$$Q_{\text{digester}} = Q_{\text{waste}} + Q_{\text{losses}} \tag{A.1}$$

$$Q_{\text{waste}} = \dot{m}_{\text{waste}} \cdot c_p \cdot \left(T_{\text{digestion}} - T_{\text{ambient}}\right) \tag{A.2}$$

$$Q_{\text{losses}} = \sum_i U_i A_i \left(T_{\text{digestion}} - T_{\text{ambient}}\right), \forall i \in \{\text{roof, walls, floor}\} \tag{A.3}$$

$$V_{\text{digester}} = \frac{\dot{m}_{\text{waste}}}{\rho_{\text{waste}}} \cdot HRT \cdot \left(1 + \frac{V_{\text{freeboard}}}{100}\right) \tag{A.4}$$

$$V_{\text{digester}} = A_{\text{floor}} \cdot \frac{D_{\text{digester}}}{D_{\text{digester}} : H_{\text{digester}}} \tag{A.5}$$

$$A_{\text{floor}} = \pi \cdot \frac{D_{\text{digester}}^2}{4} \tag{A.6}$$

$$A_{\text{wall}} = 2\pi \cdot \frac{D_{\text{digester}}}{2} \cdot \frac{D_{\text{digester}}}{D_{\text{digester}} : H_{\text{digester}}} \tag{A.7}$$

$$A_{\text{roof}} = A_{\text{floor}} \cdot \left(A_{\text{roof}} : A_{\text{floor}}\right) \tag{A.8}$$

CAPEX and OPEX estimation as a function of animal units based on data reported by the USDA (Beddoes, Bracmort, Burns, & Lazarus, 2007) is shown in Figure A.1.

Table A.1: Anaerobic digester design parameters. (Penn State Extension, 2016).

Parameter	Unit	Value
U_{floor}	W/m² K	2.85
U_{wall}	W/m² K	0.39
U_{roof}	W/m² K	0.3
V_{max}	m³	6000
$V_{freeboard}$	%	30
HRT	days	21
$D_{digester}$:$H_{digester}$	ratio	1.1
A_{roof}:A_{floor}	ratio	1.62

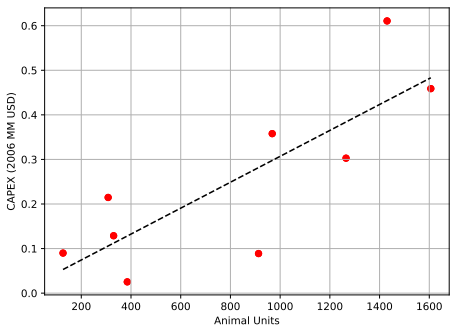

(a) Cost of AD units as a function of animal units.

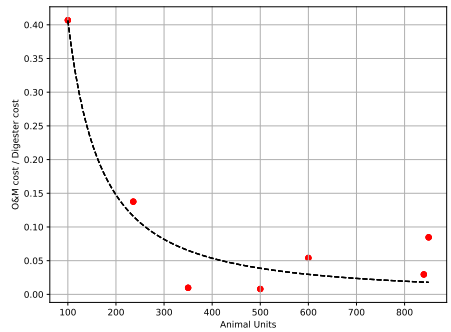

(b) O&M costs as a function of animal units.

Figure A.1: Correlations between AD capital and O&M costs, and the number of cattle in the livestock facility. Data from Beddoes, Bracmort, Burns, and Lazarus (2007).

A.1.2 *Biogas conditioning*

A.1.2.1 *Moisture removal*

The biogas produced contains saturated water at operating temperature. The first stage for water removal is the moisture condensation, which can remove residual dust and oil as well. However, the biogas moisture can remain saturated at the cooled down temperature, and additional disecation stage can be needed, using adsorbent agents such as silica gel or zeolites in packed bed columns operating at pressures between 6 and 10 bar (Ryckebosch, Drouillon, & Vervaeren, 2011).

A.1.2.2 *H_2S removal*

Hydrogen sulphide can be removed during the digestion step, or treating the biogas stream leaving the digestor. A review of H_2S can be found in Ryckebosch et al. (2011). In this work, in-biogas hydrogen sulphide removal is considered by using a fixed absorbent bed of Fe_2O_3, so that hydrogen sulphide is removed in the form of Fe_2S_3, as shown in Eq A.9. This unit operates at 25-50 ºC. Although is sensitive to the presence of water, it is a high efficient process. Therefore, the moisture removal must be previously performed.

$$Fe_2O_3 + 3H_2S \rightarrow Fe_2S_3 + 3H_2O \tag{A.9}$$

The bed can be regenerated using oxygen (air), leading to the formation of elementary sulfur, Eq. A.10.

$$2Fe_2S_3 + 3O_2 \rightarrow Fe_2O_3 + 6H_2OS \tag{A.10}$$

A.1.2.3 *Ammonia removal*

Ammonia contained in biogas can be removed by using adsorption methods such as fixed beds of zeolites or activated carbon, as well as through water scrubbing processes.

A.1.3 *Digestate solid-liquid separation*

Nutrients contained in organic waste (manure or digestate, depending on whether AD is carried out or not) are present in both organic and inorganic forms. Organic nutrients are chemically bound to carbon, and they have to be converted into their inorganic forms through a mineralization process to be available for the vegetation to grow. Organic nutrients are mainly contained in the solid phase of organic waste. Inorganic nutrients are water soluble, and they are mostly present in the liquid phase, or bounded to soluble minerals. They are immediately available to plants, including algae involved in the occurrence of algal blooms. To recover the inorganic fraction of nutrients, a solid-liquid separation stage is implemented, keeping the inorganic nutrients in the liquid stage, which will be further processed, and the organic nutrients in the solid phase, which can be composted to mineralize nitrogen and phosphorus and be further used as fertilizers.

Based on the evaluation reported by Møller, Lund, and Sommer (2000), a screw press is the technology selected to carry out the solid-liquid

separation stage since it is the most cost efficient solid-liquid separation equipment. The experimental results reported in this study are used to determine the partition coefficients for the different elements, as shown in Table A.2.

Table A.2: Partition coefficients for solid-liquid manure separation using a screw press unit (Møller, Lund, & Sommer, 2000)

Element	Solid fraction	Liquid fraction
Total mass	0.08	0.92
Dry matter	0.31	0.69
Org. N	0.09	0.91
Org. P	0.22	0.78

To determine the commercial sizes and number of units necessary as a function of the flow to be treated, data from commercial manufacturers is considered (PWTech, 2018). The feasible configurations in terms of screw press diameter and number of units as a function of the waste flow treated are shown in Table 4 of the Supplementary Material. Data reported by Matches (2014) for this type of equipment is used to relate the unit diameter and cost, while the operating costs are calculated assuming power consumption reported by the manufacturer for each model, as shown in Fig. A.2 and Tables A.3 and A.4.

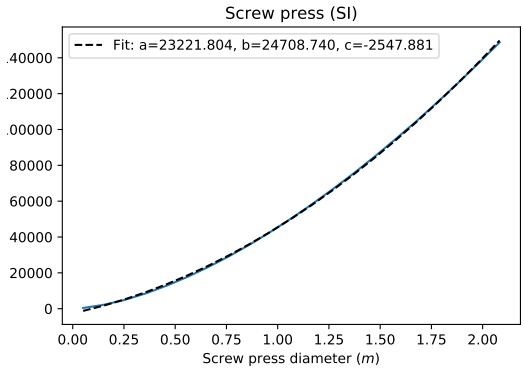

Figure A.2: Estimated screw press investment costs (USD) as a function of the size.

Assuming the discretization of units due to the commercial sizes available, the investment and operating costs for the screw press equipment are presented in Fig 4 of the Supplementary Material.

Table A.3: Sizing estimated for screw press units based on commercial data (PWTech, 2018)

Load capacity $\left(\frac{m^3}{day}\right)$	Number of units			
	⌀(m) 0.23	⌀(m) 0.35	⌀(m) 0.42	⌀(m) 0.56
< 43	1	-	-	-
43 - 81	-	1	-	-
81 - 190	-	-	1	-
190 - 381	-	-	2	-
381 - 572	-	-	3	-
572 - 708	-	-	-	2
708 - 1090	-	-	-	3
1090 - 1444	-		-	4
> 1444	-	-	-	$\left\lceil \frac{\text{Flow } (m^3/day)}{\text{Load Capacity}_{\text{⌀0.56m unit}}} \right\rceil$

Table A.4: Electrical power of screw press units (PWTech, 2018)

Number of units	Electrical power (kW)			
	⌀(m) 0.23	⌀(m) 0.35	⌀(m) 0.42	⌀(m) 0.56
1	0.3	0.45	0.9	-
2	-	-	1.27	3.88
3	-	-	2.01	6.34
4	-	-	-	7.83

A.1.4 *Struvite production: Multiform system*

Struvite production from livestock waste has been estimated based on a detailed thermodynamic model for precipitates (struvite and calcium compounds) formation considering the main chemical systems involved in the formation of precipitates, shown in Tables A.5 and A.6. pK denotes the thermodynamic equilibrium constant, and pK_{sp} refers to the solubility product. The variability in the organic waste composition is also considered, obtaining surrogate models to predict the formation of struvite based on different waste parameters, including the concentration of magnesium, the concentration of calcium, and the alkalinity level (Martín-Hernández, Ruiz-Mercado, & Martín, 2020). Based on previous studies, the supply of magnesium has been fixed at a $Mg^{2+}/PO^{3-}{}_4$ molar ratio of 2, estimating the

formation of struvite as a function of the concentration of Ca^{2+} ions, which compete for phosphate ions hindering the formation of struvite, shown in Eq. A.11. A comprehensive description of the thermodynamic model used for the development of the correlations to estimate the formation of struvite can be found in Martín-Hernández et al. (2020).

Table A.5: Aqueous phase chemical systems considered in the thermodynamic model for estimating the formation of struvite.

Name	Chemical system	pK	Source
Ammonia	$NH_4^+ \leftrightarrow NH_3 + H^+$	9.2	(Bates & Pinching, 1949)
Water	$H_2O \leftrightarrow OH^- + H^+$	14	(Skoog, West, Holler, & Crouch, 2014)
Phosphoric acid	$H_3PO_4 \leftrightarrow H_2PO_4^- + H^+$	2.1	(Ohlinger, Young, & Schroeder, 1998)
	$H_2PO_4^- \leftrightarrow HPO_4^{2-} + H^+$	7.2	(Ohlinger, Young, & Schroeder, 1998)
	$HPO_4^{2-} \leftrightarrow PO_4^{3-} + H^+$	12.35	(Ohlinger, Young, & Schroeder, 1998)
Carbonic acid	$H_2CO_3 \leftrightarrow HCO_3^- + H^+$	6.35	(Skoog, West, Holler, & Crouch, 2014)
	$HCO_3^- \leftrightarrow CO_3^{2-} + H^+$	10.33	(Skoog, West, Holler, & Crouch, 2014)

Table A.6: Solids species considered in the thermodynamic model for estimating the formation of struvite.

Name	Chemical system	pK_{sp}	Source
Struvite	$MgNH_4PO_4 \cdot 6H_2O \leftrightarrow Mg^{2+} + NH_4^+ + PO_4^{3-}$	13.26	(Ohlinger, Young, & Schroeder, 1998)
K-struvite	$MgKPO_4 \cdot 6H_2O \leftrightarrow Mg^{2+} + K^+ + PO_4^{3-}$	10.6	(Taylor, Frazier, & Gurneynium, 1963)
Hydroxyapatite	$Ca_5(PO_4)_3OH \leftrightarrow 5Ca^{2+} + 3PO_4^{3-} + OH^-$	44.33	(Brezonik & Arnold, 2011)
Calcium carbonate	$CaCO_3 \leftrightarrow Ca^{2+} + CO_3^{2-}$	8.48	(Morse, Arvidson, & Lüttge, 2007)
Tricalcium phosphate	$Ca_3(PO_4)_2 \leftrightarrow 3Ca^{2+} + 2PO_4^{3-}$	25.50	(Fowler & Kuroda, 1986)
Dicalcium phosphate	$CaHPO_4 \leftrightarrow Ca^{2+} + HPO_4^{2-}$	6.57	(Gregory, Moreno, & Brown, 1970)
Calcium hydroxide	$Ca(OH)_2 \leftrightarrow Ca^{2+} + 2OH^-$	5.19	(Skoog, West, Holler, & Crouch, 2014)
Magnesium hydroxide	$Mg(OH)_2 \leftrightarrow Mg^{2+} + 2OH^-$	11.15	(Skoog, West, Holler, & Crouch, 2014)

A correlation to estimate the formation of struvite through the fraction of phosphorus recovered as struvite $\left(x_{\text{struvite}\left(PO_4^{3-}\right)}\right)$ as a function of calcium concentration in the waste has been used in this work, Eq. A.11 (Martín-Hernández et al., 2020). Based on the correlation shown in Eq. A.11, the amount of nitrogen recovered is estimated through Eq. A.13.

$$x_{\text{struvite}\left(PO_4^{3-}\right)} = \frac{0.798}{1 + \left(x_{Ca^{2+}:PO_4^{3-}} \cdot 0.576\right)^{2.113}} \tag{A.11}$$

$$\dot{m}_{\text{struvite } recovered} = \dot{m}_{\text{P } in} \cdot x_{\text{struvite}\left(PO_4^{3-}\right)} \cdot \frac{MW_{\text{struvite}}}{MW_{\text{P}}} \tag{A.12}$$

$$\dot{m}_{\text{N } recovered} = \dot{m}_{\text{struvite } recovered} \cdot \frac{MW_{\text{N}}}{MW_{\text{struvite}}} \tag{A.13}$$

$$\dot{m}_{\text{N } released} = \dot{m}_{\text{N } in} - \dot{m}_{\text{struvite } recovered} \cdot \frac{MW_{\text{N}}}{MW_{\text{struvite}}} \tag{A.14}$$

A.1.5 *MAPHEX*

The mass balances of MAPHEX process are shown in Eqs. A.15-A.19, based on experimental data for full-scale modular units reported by Church et al. (2018).

$$\dot{m}_{nutrients_{\text{recovered}}} = \dot{m}_{nutrients,\ in} \cdot \eta_{\text{MAPHEX}}^{nutrients} \ \forall\ nutrients \in \{\text{P, N}\} \tag{A.15}$$

$$\dot{m}_{nutrients_{\text{released}}} = \dot{m}_{nutrients,\ in} \cdot \left(1 - \eta_{\text{MAPHEX}}^{nutrients}\right) \ \forall\ nutrients \in \{\text{P, N}\} \tag{A.16}$$

$$\dot{m}_{\text{TS}_{\text{recovered}}} = \dot{m}_{\text{TS},in} \cdot 0.93 \tag{A.17}$$

$$\dot{m}_{\text{water}_{\text{recovered}}} = \frac{\dot{m}_{\text{TS}_{\text{recovered}}}}{0.25} \cdot 0.75 \tag{A.18}$$

$$\dot{m}_{\text{water}_{\text{released}}} = \dot{m}_{\text{water},in} - \dot{m}_{\text{water}_{\text{recovered}}} \tag{A.19}$$

A.1.6 *Transmembrane chemisorption*

Characteristics of Liquid-Cel™ Extra Flow membranes are shown in Table A.7. Membrane modules cost are illustrated in Figure A.3.

The main parameters for membrane modeling are collected in Eqs. A.20-A.33. Digestate density (ρ) and (μ) viscosity were assumed equal to those of water. Correlations to estimate these parameters are reported by Hsu and Li (1997). Ammonia Henry's constant (H_{NH_3}) have been taken from Linstrom and Mallard (2001).

Table A.7: Main characteristics of Liquid-Cel ™ membrane (Rongwong & Sairiam, 2020; Ulbricht, Schneider, Stasiak, & Sengupta, 2013).

Membrane parameters	Unit	Variable	Values
Number of fibers	$\frac{\text{fibers}}{\text{m}^2_{\text{module}}}$	n_f	$2.13 \cdot 10^6$
Fiber outer diameter	m	d_o	$300 \cdot 10^{-6}$
Fiber inner diameter	m	d_i	$240 \cdot 10^{-6}$
Pore diameter	m	a	$0.04 \cdot 10^{-6}$
Porosity	-	ε	0.40
Tortuosity factor	-	τ	2.60
Pressure drop shell side	bar	$\Delta P_{\text{shell side}}$	0.3
Pressure drop lumen side	bar	$\Delta P_{\text{lumen side}}$	2

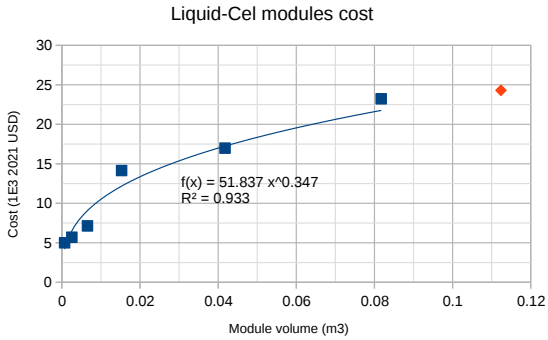

Figure A.3: Estimation of Liquid-Cel™ 14x40 membrane module cost.

$$\rho_{\text{water}}\left(\frac{\text{kg}}{\text{m}^3}\right) = (10^3)\cdot \left(0.863559 + 1.21494 \cdot 10^{-3} \cdot T(\text{K}) - 2.5708 \cdot 10^{-6} \cdot T(\text{K})^2\right) \tag{A.20}$$

$$\mu_{\text{water}}\left(\frac{\text{kg}}{\text{m} \cdot \text{s}}\right) = (10^{-6}) \cdot \left(\rho \cdot e^{-3.28285 + \frac{456.029}{T(\text{K}) - 154.576}}\right) \tag{A.21}$$

$$H_{\text{NH}_3}\left(\frac{\text{kmol}}{\text{atm} \cdot \text{m}^3}\right) = 58 \cdot e^{4100 \cdot \left(\frac{1}{T(\text{K})} - \frac{1}{298.15}\right)} \tag{A.22}$$

The cross-sectional area of the lumen area is calculated based on the transverse area of hollow fiber, and the number of fibers in the membrane module, Eq. A.24 . Shell area is calculated as the difference between total and lumen side cross-sectional areas. Velocities of digestate and stripping

fluid (i.e., sulfuric acid solution) are computed based on their respective volumetric flow and transverse areas.

$$n_{f_{\text{module}}} = A_{\text{module}} \cdot n_f \tag{A.23}$$

$$A_{\text{lumen side}}\left(\text{m}^2\right) = \frac{d_i^2}{4} \cdot \pi \cdot n_{f_{\text{module}}} \tag{A.24}$$

$$A_{\text{shell side}}\left(\text{m}^2\right) = \frac{D_{\text{module}^2}}{4} \cdot \pi - A_{\text{lumen side}} \tag{A.25}$$

$$V_{\text{stripping fluid}}\left(\frac{\text{m}}{\text{s}}\right) = \frac{\dot{V}_{\text{stripping fluid}}}{A_{\text{lumen side}}} \tag{A.26}$$

$$V_{\text{digestate}}\left(\frac{\text{m}}{\text{s}}\right) = \frac{\dot{V}_{\text{digestate}}}{A_{\text{shell side}}} \tag{A.27}$$

Diffusion of ammonia through the membrane is driven by bulk and Knudsen diffusivities, which consider the mean free path of molecules and the pore diameter respectively. Bulk diffusivity of ammonia is calculated based on the kinetic theory, using Eq. A.29, while Knudsen diffusivity depends on the molecular velocity, Eq. A.28, and pore diameter, Eq. A.31 Agrahari, Shukla, Verma, and Bhattacharya (2012). Both contributions to ammonia transport are combined in an effective diffusion coefficient, Eq. A.32. Ammonia diffusion in liquid phase has been assumed equal to ammonia diffusion in water, which is calculated using Eq. A.33.

$$\bar{v}\left(\frac{\text{m}}{\text{s}}\right) = \left(\frac{8 \cdot R\left(\frac{\text{J}}{\text{mol}\cdot\text{K}}\right) \cdot T\,(\text{K})}{MW_{\text{NH}_3}\left(\frac{\text{kg}}{\text{mol}}\right) \cdot \pi}\right)^{1/2} \tag{A.28}$$

$$D_{\text{NH}_3}\left(\frac{\text{m}^2}{\text{s}}\right) = \frac{1}{3} \cdot \lambda \cdot \bar{v} \tag{A.29}$$

$$\lambda\,(\text{m}) = \frac{\kappa\left(\frac{\text{J}}{\text{K}}\right) \cdot T\,(\text{K})}{\pi \cdot \sigma_{\text{NH}_3}^2\,(\text{m}^2) \cdot P\,(\text{Pa}) \cdot 2^{1/2}} \tag{A.30}$$

$$D_{\text{NH}_{3\text{Kn}}}\left(\frac{\text{m}^2}{\text{s}}\right) = \frac{d_{\text{pore}}}{3} \cdot \left(\frac{8 \cdot R\left(\frac{\text{J}}{\text{mol}\cdot\text{K}}\right) \cdot T(\text{K})}{\pi \cdot MW_{\text{NH}_3}\left(\frac{\text{kg}}{\text{mol}}\right)}\right)^{1/2} \tag{A.31}$$

$$D_{\text{eff}}\left(\frac{\text{m}^2}{\text{s}}\right) = \frac{1}{\frac{1}{D_{\text{NH}_{3\text{Kn}}}} + \frac{1}{D_{\text{NH}_3}}} \tag{A.32}$$

$$D_{\text{NH}_{3\text{water}}}\left(\frac{\text{m}^2}{\text{s}}\right) = 1.96 \cdot 10^{-9} \cdot \frac{\mu_{\text{water}_{T=298\text{K}}}}{\mu_{\text{water}_T}} \cdot \frac{T\,(\text{K})}{298} \tag{A.33}$$

The distribution of ammonia species shown in Eq. 3.10 is calculated at initial conditions based on the pH of the digestate stream being fed through the tube side of the membrane module, which is assumed equal to 11, as shown in Eqs. A.34-A.38.

$$f_{NH_3} = \frac{1}{10^{\left(pK_{a_{NH_3}} - pH\right)} + 1} \tag{A.34}$$

$$pK_{a_{NH_3}}\left(\frac{\text{kmol}}{\text{m}^3}\right) = 0.0901821 + \frac{2729.92}{T(\text{K})} \tag{A.35}$$

$$[NH_3] = [N_{inorg}] \cdot f_{NH_3} \tag{A.36}$$

$$[NH_4^+] = [N_{inorg}] \cdot (1 - f_{NH_3}) \tag{A.37}$$

$$[H^+] = K_a \cdot \frac{[NH_4^+]}{[NH_3]} \tag{A.38}$$

A modified Henry's constant considering the speciation of ammonia is used in the model proposed by Rongwong and Sairiam (2020) to evaluate the liquid-solid equilibrium of ammonia, Eq. A.39.

$$H^*_{NH_3} = H_{NH_3} \cdot \left(1 + \frac{K_a \cdot [H^+]}{Kw}\right) \tag{A.39}$$

The mass transfer coefficient of the digestate flowing in the tube side, $k_{\text{digestate}}$, is calculated through the Sherwood number of this stream, Eq. A.40.

$$\text{Sh}_{\text{digestate}} = \frac{k_{\text{digestate}} \cdot d_i}{D_{NH_{3_{\text{water}}}}} = 1.62 \cdot \left(\frac{d_i}{L} \cdot \text{Re}_{\text{digestate}} \cdot \text{Sc}_{\text{digestate}}\right)^{1/3} \tag{A.40}$$

$$\text{Re}_{\text{digestate}} = \frac{d_i \cdot \rho_{\text{digestate}} \cdot V_{\text{digestate}}}{\mu_{\text{digestate}}} \tag{A.41}$$

$$\text{Sc}_{\text{digestate}} = \frac{\mu_{\text{digestate}}}{\rho_{\text{digestate}} \cdot D_{NH_{3_{\text{water}}}}} \tag{A.42}$$

The membrane phase can be divided into non-wetted and wetted membrane sections. Their mass transfers coefficients, k_M and k'_M respectively, are calculated based on the fraction of membrane wetted by the digestate. This is calculated based on a correlation reported by Rongwong and

Sairiam (2020), shown in Eq. A.43. Eqs. A.45-A.46 and A.47-A.48 shown the equations employed for the estimation of k_M and k'_M respectively.

$$w_{\text{membrane}} = \frac{0.368}{2.709 + e^{-17.486 \cdot \left(V_{\text{digestate}} - 0.25\right)}} \tag{A.43}$$

$$d_{\text{interfacial}}\,(\text{m}) = d_i + w_{\text{membrane}} \cdot (d_o - d_i) \tag{A.44}$$

$$k_M \left(\frac{\text{m}}{\text{s}}\right) = \frac{D_{\text{eff}} \cdot \varepsilon}{\tau \cdot \delta_{\text{non-wetted}}} \tag{A.45}$$

$$\delta_{\text{non-wetted}}\,(\text{m}) = \frac{d_o - d_{\text{interfacial}}}{2} \tag{A.46}$$

$$k'_M \left(\frac{\text{m}}{\text{s}}\right) = \frac{D_{\text{water}} \cdot \varepsilon}{\tau \cdot \delta_{\text{wetted}}} \tag{A.47}$$

$$\delta_{\text{wetted}}\,(\text{m}) = \frac{d_{\text{interfacial}} - d_i}{2} \tag{A.48}$$

The overall mass transfer coefficient is calculated based on the liquid, wetted membrane, and non-wetted membranes mass transfer coefficients, as shown in Eq. A.49. However, high ammonia concentrations result in a decrease of the overall mass transfer (Zhu, Hao, Shen, & Chen, 2005). Therefore, K_{ov} is modified using a correction factor that consider the concentration of ammonia in digestate.

$$K_{ov} \left(\frac{\text{m}}{\text{s}}\right) = \frac{1}{\left(\frac{1}{k_{\text{digestate}} \cdot d_i} + \frac{1}{k'_M \cdot \delta_{\ln\text{ wetted}}} + \frac{R\left(\frac{\text{atm}\cdot\text{m}^3}{\text{kmol}\cdot\text{K}}\right) \cdot T(\text{K}) \cdot H^*_{\text{NH}_3}}{k_M \delta_{\ln\text{ non-wetted}}}\right) \cdot d_o} \tag{A.49}$$

$$\delta_{\ln\text{ wetted}} = \frac{d_{\text{interfacial}} - d_i}{\ln\left(\frac{d_{\text{interfacial}}}{d_i}\right)} \tag{A.50}$$

$$\delta_{\ln\text{ non-wetted}} = \frac{d_o - d_{\text{interfacial}}}{\ln\left(\frac{d_o}{d_{\text{interfacial}}}\right)} \tag{A.51}$$

$$K_{ov_{\text{corrected}}} \left(\frac{\text{m}}{\text{s}}\right) = K_{ov} \cdot \left(1 - \frac{0.002728 \cdot [\text{NH}_3]\,\left(\frac{\text{mg}}{\text{L}}\right)}{100}\right) \tag{A.52}$$

The mass balance along the membrane can be performed considering the mass transfer in an infinitesimal element of the membrane, as shown in Eq. A.53. Due to the excess of sulfuric acid in the lumen side that lead to the formation of ammonium sulfate from the ammonia recovered, the concentration of ammonia in the lumen side is assumed negligible. This differential expression can be analytically integrated to estimate the total length of the membrane, Eq. A.54.

$$\frac{\dot{n}_{NH_3}}{dz} = -n_{f_{module}} \cdot \pi \cdot d_o \cdot K_{ov_{corrected}} \cdot \left(\frac{\dot{n}_{NH_3}}{\dot{V}_{digestate}} - \frac{H^*_{NH_3} \cdot p_{NH_3}}{\dot{V}_{digestate}} \right)$$

$$\approx -n_{f_{module}} \cdot \pi \cdot d_o \cdot K_{ov_{corrected}} \cdot \frac{\dot{n}_{NH_3}}{\dot{V}_{digestate}} \tag{A.53}$$

$$z\,(\mathrm{m}) = \ln\left(\frac{\dot{n}_{NH_{3_{final}}}}{\dot{n}_{NH_{3_{initial}}}} \right) \cdot \frac{\dot{V}_{digestate}}{-n_{f_{module}} \cdot \pi \cdot d_o \cdot K_{ov_{corrected}}} \tag{A.54}$$

Pumps to drive the digestate and stripping fluid streams are needed. Their cost is estimated using Eqs. A.55 and A.56, assuming that the maximum capacity of one single pump $\left(\dot{V}_{pump_{max}}\right)$ is 1 m^3/s (Peters, Timmerhaus, West, et al., 2003). Pumps operating cost are estimated through Eqs. A.57 to A.59, calculating the energy needed to balance the pressure drop of the shell and lumen sides of the membrane, Table A.7. Pump efficiencies $\left(\eta_{pump_i}\right)$ of 0.8 are assumed.

$$n_{pump_i} = \left\lceil \frac{\dot{V}_i}{\dot{V}_{pump_{max}}} \right\rceil \tag{A.55}$$

$$CAPEX_{pumps_i}\,(2019\ \mathrm{USD}) =$$

$$\begin{cases} (-50.387 \cdot 10^6 \cdot \dot{V}_i^2 + 1.607 \cdot 10^6 \cdot \dot{V}_i & \\ +5.127 \cdot 10^3) \cdot n_{pump_i} \cdot 1.055 & \text{if } \dot{V}_i \leq 9 \cdot 10^{-3}\,\frac{m^3}{s} \\ (92.562 \cdot 10^3 \cdot \dot{V}_i^{0.381}) \cdot n_{pump_i} \cdot 1.055 & \text{if } \dot{V}_i > 9 \cdot 10^{-3}\,\frac{m^3}{h} \end{cases} \tag{A.56}$$

$$H_i\,(\mathrm{m}) = \frac{\Delta P_i\,(\mathrm{Pa})}{\rho\left(\frac{kg}{m^3}\right) g\left(\frac{m}{s^2}\right)} \tag{A.57}$$

$$\dot{W}_{pump_i}\,(\mathrm{kW}) = \frac{g\left(\frac{m}{s^2}\right) \cdot H_i\,(\mathrm{m}) \cdot \rho\left(\frac{kg}{m^3}\right) \cdot \dot{V}_i\left(\frac{m^3}{s}\right)}{\eta_{pump_i}} \tag{A.58}$$

$$OPEX_{pumps}\left(\frac{2019\ \mathrm{USD}}{\mathrm{year}}\right) = \sum_i \dot{W}_{pump_i}\,(\mathrm{kW}) \cdot t_{operation}\,(\mathrm{s}) \cdot 3600$$

$$\cdot\, Price_{electricity}\left(\frac{\mathrm{USD}}{\mathrm{kWh}}\right) \tag{A.59}$$

$$\forall\ i \in \{\text{shellside, lumenside}\}$$

A.1.7 *Ammonia evaporation*

The following assumptions have been made for the modeling of digestate drying:

- $c_{p_{\text{digestate}_{\text{in}}}} \approx c_{p_{\text{water}}}$
- $P_{\text{water}} + P_{NH_3} \approx P_{\text{water}}$
- $T_{\text{out}_{\text{air}}} = T_{\text{out}_{\text{digestate}}}$
- $\alpha = \text{constant}$

The mass and energy balances for digestate drying in a belt dryer unit are shown in Eqs. A.60-A.62 and A.63-A.72 respectively

$$\dot{m}_{NH_3\,\text{evap}} = \dot{m}_{NH_3\,\text{in}} \cdot \eta^{NH_3}_{\text{belt dryer}} \tag{A.60}$$

$$\frac{\frac{\dot{m}_{\text{water}_{\text{evap}}}}{MW_{\text{water}}}}{\sum_j \frac{\dot{m}_j}{MW_j}} \cdot P_{\text{total}} \leq Pv_{\text{water}}(T) \;\forall\; j \in \{\text{air},\ H_2O,\ NH_3\} \tag{A.61}$$

$$\frac{\frac{\dot{m}_{NH_3\,\text{evap}}}{MW_{NH_3}}}{\sum_j \frac{\dot{m}_j}{MW_j}} \leq Pv_{NH_3}(T) \;\forall\; j \in \{\text{air},\ H_2O,\ NH_3\} \tag{A.62}$$

$$\dot{Q}_{\text{Belt Dryer}} = \dot{H}_{\text{latent}} + \dot{H}_{\text{sensible}} = \dot{H}_{\text{air}_{\text{in}}} - \dot{H}_{\text{air}_{\text{out}}} \tag{A.63}$$

$$\dot{H}_{\text{latent}} = \dot{m}_{\text{water}_{\text{evap}}} \cdot \lambda_{\text{evap}_{\text{water}}}(T) + \dot{m}_{NH_{3_{\text{evap}}}} \cdot \lambda_{\text{evap}_{NH_3}}(T) \tag{A.64}$$

$$\dot{H}_{\text{sensible}} = \dot{H}_{\text{digestate}_{\text{out}}} - \dot{H}_{\text{digestate}_{\text{in}}} + \dot{H}_{\text{sensible}_{\text{gases}}} \tag{A.65}$$

$$\dot{H}_{\text{sensible}_{\text{gases}}} = \left(\dot{m}_{\text{water}_{\text{evap}}} + \dot{m}_{NH_{3_{\text{evap}}}}\right) \cdot c_{p_{\text{water (liquid)}}} \cdot T_{\text{air}_{\text{out}}} \tag{A.66}$$

$$\dot{H}_{\text{digestate}_{\text{in}}} = \dot{m}_{\text{digestate}_{\text{in}}} \cdot c_{p_{\text{water}}} \cdot \Delta T_{\text{digestate}_{\text{in}}} \tag{A.67}$$

$$\dot{H}_{\text{digestate}_{\text{out}}} = \dot{m}_{\text{digestate}_{\text{out}}} \cdot c_{p_{\text{digestate}}} \cdot \Delta T_{\text{digestate}_{\text{out}}} \tag{A.68}$$

$$c_{p_{\text{digestate}}}\left(kg/kJ \cdot K\right) = 4.19 - 0.0275 \cdot \left(\frac{\dot{m}_{\text{TS}_{\text{out}}}}{\dot{m}_{\text{digestate}_{\text{out}}}} \cdot 100\right) \tag{A.69}$$

$$\dot{H}_{\text{air}_{\text{in}}} = \dot{m}_{\text{air}} \cdot c_{p_{\text{air}}} \cdot \Delta T_{\text{air}_{\text{in}}} \tag{A.70}$$

$$\dot{H}_{\text{air}_{\text{out}}} = \left(\dot{m}_{\text{air}} \cdot c_{p_{\text{air}}} + \dot{m}_{\text{water}_{\text{evap}}} \cdot c_{p_{\text{water (gas)}}} + \dot{m}_{NH_{3_{\text{evap}}}} \cdot c_{p_{NH_3\,\text{(gas)}}}\right) \cdot \Delta T_{\text{air}_{\text{out}}} \tag{A.71}$$

$$\Delta T_i = T_i - T_{\text{ref}} \;\forall\; i \in \{\text{air}_{\text{in}},\ \text{air}_{\text{out}},\ \text{digestate}_{\text{in}},\ \text{digestate}_{\text{out}}\} \tag{A.72}$$

A.1.8 *Stripping in packed tower*

The liquid mass velocity is a known parameter since it corresponds to the digestate being processed. The gas velocity is estimated by combining Eqs. 3.23, **??** and 3.27. The design gas mass velocity considered is 0.7 time

the gas mass velocity, Eq 3.28, while the liquid design mass velocity is computed by combining Eqs. 3.28 and 3.27. Tower diameter is computed based on the design liquid mass velocity and liquid mass flow. However, design restrictions reported by (Branan, 2005) have been considered in the sizing of the packed tower. Tower height is estimated through the height and number of transfer units, Eqs A.73 and A.74. Therefore, the design diameter is computed as shown in Eqs. A.75 to A.77. Additionally, the number of packed towers that have to be installed in-parallel arrangement is estimated through Eq. A.78.

$$D_{\text{design}} \leq 1.2 \text{ m} \tag{A.73}$$

$$\frac{H_{\text{design}}}{D_{\text{design}}} \leq 30 \tag{A.74}$$

$$A_{\text{stripping tower}} = \frac{\dot{m}_L}{G_{L_{\text{design}}}} \tag{A.75}$$

$$D_{\text{stripping tower}} = \left(\frac{A_{\text{stripping tower}}}{\pi} \right)^{0.5} \tag{A.76}$$

$$D^{\text{design}}_{\text{stripping tower}}\,(\text{m}) = \begin{cases} D_{\text{stripping tower}} & \text{if } D_{\text{stripping tower}} \leq 1.2 \text{ m} \\ 1.2 & \text{if } D_{\text{scrubber}} > 1.2 \text{ m} \end{cases} \tag{A.77}$$

$$n^{\text{parallel}}_{\text{stripping tower}} = \left\lceil \frac{D_{\text{stripping tower}}(\text{m})}{1.2} \right\rceil \tag{A.78}$$

The height of the stripping packed towers is estimated through the height and number of transfer units, Eq. A.79 and A.80 respectively (Metcalf & Eddy, 2014). The liquid overall mass transfer coefficient value assumed for the ammonia air system is 2 h^{-1} (Larsen, Udert, & Lienert, 2013). The design restriction shown in Eq. A.74 is considered to compute the design height of the stripping towers, and the number of units that must be installed in series, Eq. A.83.

$$HTU = \frac{\frac{\dot{m}_L}{n^{\text{parallel}}_{\text{stripping tower}} \cdot \rho_{\text{digestate}}}}{K_L a \cdot \pi \cdot \left(\frac{D_{\text{stripping tower}}}{2}\right)^2} \tag{A.79}$$

$$NTU = \frac{S}{S-1} \ln\left(\frac{\frac{1}{1-\eta_{\text{stripping tower}}/100} \cdot (S-1)+1}{S}\right) \tag{A.80}$$

$$S = \frac{H_{NH_3}}{P_{\text{stripping tower}}} \cdot \frac{\dot{m}_G}{\dot{m}_L} \tag{A.81}$$

$$H_{\text{stripping tower}} = NTU \cdot HTU \tag{A.82}$$

$$n^{\text{series}}_{\text{stripping tower}} = \left\lceil \frac{\frac{H_{\text{stripping tower}}}{D^{\text{design}}_{\text{stripping tower}}}}{30} \right\rceil \tag{A.83}$$

$$H^{\text{design}}_{\text{stripping tower}}\,(\text{m}) = \begin{cases} H_{\text{stripping tower}} & \text{if } \frac{H_{\text{stripping tower}}}{D_{\text{stripping tower}}} \leq 30 \\ \frac{\frac{\dot{m}_L}{n^{\text{series}}_{\text{stripping tower}} \cdot n^{\text{parallel}}_{\text{stripping tower}} \cdot \rho_{\text{digestate}}}}{K_L a \cdot \pi \cdot \left(\frac{D_{\text{stripping tower}}}{2}\right)^2} & \text{if } \frac{H_{\text{stripping tower}}}{D_{\text{stripping tower}}} \leq 30 \end{cases} \tag{A.84}$$

A.1.9 *Acidic scrubbing*

Mass balances to scrubber unit consider the water transferred to the gas stream, assuming that saturation is reached, Eq. A.86. Ammonia recovery efficiency ($\eta^{NH_3}_{scrubber}$) of full-scale ammonia scrubbers has been reported in the range of 40% to 99% (Melse & Ogink, 2005). A typical $\eta^{NH_3}_{scrubber}$ of 96% has been selected based on the work of Melse and Ogink (2005).

$$\frac{P_{\text{water}}}{Pv_{\text{water}}} = 1 \tag{A.85}$$

$$Pv_{\text{water}} = \frac{\frac{\dot{m}^{\text{gas stream}}_{\text{water}_{out}}}{MW_{\text{water}}}}{\sum_j \frac{\dot{m}^{\text{gas stream}}_{\text{j}}}{MW_{\text{j}}}} \cdot P^{\text{gas stream}}_{in} \tag{A.86}$$

$$\dot{m}^{\text{gas stream}}_{NH_3\ out} = \dot{m}^{\text{gas stream}}_{NH_3\ in} \cdot \left(1 - \eta^{NH_3}_{scrubber}\right) \tag{A.87}$$

The water flow needed to perform the scrubbing operation is computed from the operation line of the unit (L/G), Eq. A.88. Following the rules of thumb for scrubbing units, the design operation line has been assumed as twice the minimum operation line, Eq. A.89. Y_{NH_3} and X_{NH_3} denote

the ammonia free basis molar fractions in gas and liquid streams respectively. The amount of sulfuric acid supplied to make-up the sulfate used for ammonium sulfate formation, Eq. A.91, is slightly larger than the stoichiometric amount of the precipitation reaction, 3.5 $kg_{H_2SO_4}$ per kg_{NH_3} recovered (Bolzonella, Fatone, Gottardo, & Frison, 2018).

$$(L/G)_{\text{min}} = \frac{Y_{NH_{3in}} - Y_{NH_{3out}}}{X_{NH_{3out}} - X_{NH_{3in}}} \tag{A.88}$$

$$(L/G) = (L/G)_{\text{min}} \cdot 2 \tag{A.89}$$

$$\dot{m}^{\text{liquid stream}}_{\text{water}_{in}} = \left((L/G) \cdot \dot{n}^{\text{liquid stream}}_{\text{total}_{in}} - \dot{n}^{\text{liquid stream}}_{NH_3\ in} \right) \cdot MW_{\text{water}} \tag{A.90}$$

$$\dot{m}^{\text{liquid stream}}_{H_2SO_{4_{in}}} = \dot{m}^{\text{gas stream}}_{NH_3\ in} \cdot \eta^{NH_3}_{scrubber} \cdot 3.5 \tag{A.91}$$

$$\dot{m}^{\text{liquid stream}}_{(NH_4)_2SO_{4_{out}}} = \frac{\dot{m}^{\text{gas stream}}_{NH_3\ in} \cdot \eta^{NH_3}_{scrubber}}{MW_{NH_3}} \cdot MW_{(NH_4)_2SO_{4_{out}}} \tag{A.92}$$

The scrubber diameter, Eq. A.94, is based on the gas velocity in the equipment, which is assumed equal to 1.75 m/s (Melse & Ogink, 2005). The number of units is set by the maximum diameter of scrubbers, Eq. A.95, which is assumed equal to 1.2 m according to the rules of thumb for packed columns (Branan, 2005).

$$D_{\text{scrubber}}\,(\text{m}) = \frac{\dot{V}^{\text{gas stream}}\left(\frac{\text{m}^3}{\text{s}}\right)}{1.75\left(\frac{\text{m}}{\text{s}}\right)} \tag{A.93}$$

$$D^{\text{design}}_{\text{scrubber}}\,(\text{m}) = \begin{cases} D_{\text{scrubber}} & \text{if } D_{\text{scrubber}} \leq 1.2 \text{ m} \\ 1.2 & \text{if } D_{\text{scrubber}} > 1.2 \text{ m} \end{cases} \tag{A.94}$$

$$n_{\text{scrubbers}} = \left\lceil \frac{\dot{V}^{\text{gas stream}}\left(\frac{\text{m}^3}{\text{s}}\right)}{1.75\left(\frac{\text{m}}{\text{s}}\right) \cdot \frac{1.2^2(\text{m}^2)}{4}\pi} \right\rceil \tag{A.95}$$

The height of scrubbing units is estimated through the height and number of transfer units, Eq. A.96, as described by Couper, Penney, Fair, and Walas (2005). The number of transfer units is determined by the Kremser shortcut method, as shown in Eq. A.97 (Seader, Seider, & Lewin, 2004), while the height of each transfer unit is calculated in Eq. A.101. The gas film overall mass transfer coefficient value for the ammonia air system is 272474.56 $\frac{\text{mol}}{\text{h}\cdot\text{m}^3\cdot\text{atm}}$ (Branan, 2005). The scrubbing operation involves the use of compressors for pumping the stripping gas stream. The energy required for compression is estimated though Eq. A.102, assuming a compressor efficiency $(\eta_{\text{compressor}})$ of 0.85 and a polytropic coefficient (k) of 1.4. The

pressure drop of a typical scrubber for ammonia capture assumed is 200 Pa (Melse & Ogink, 2005).

$$H_{\text{scrubber}} = NTU \cdot HTU \tag{A.96}$$

$$NTU = \frac{\ln\left(\left(1 - m \cdot \frac{\dot{n}^{\text{gas stream}}}{\dot{n}^{\text{liquid stream}}}\right) \frac{x^{\text{gas stream}}_{\text{NH}_{3in}} - x^{*}_{\text{NH}_3}}{x^{\text{gas stream}}_{\text{NH}_{3out}} - x^{*}_{\text{NH}_3}} + m \cdot \frac{\dot{n}^{\text{gas stream}}}{\dot{n}^{\text{liquid stream}}}\right)}{\ln\left(m \cdot \frac{L}{V}\right)} \tag{A.97}$$

$$x^{\text{gas stream}}_{\text{NH}_{3k}} = \frac{\dot{n}^{\text{gas stream}}_{\text{NH}_{3k}}}{\dot{n}^{\text{gas stream}}}, \; \forall \; k \; \in \; \{in, out\} \tag{A.98}$$

$$x^{*}_{\text{NH}_3} = 0 \tag{A.99}$$

$$m = \frac{P_{\text{NH}_3}}{P} \tag{A.100}$$

$$HTU = \frac{\dot{n}^{\text{gas stream}}\left(\frac{\text{mol}}{\text{h}}\right)}{\pi \cdot \frac{D^{\text{design}^2}_{\text{scrubber}}}{4}\left(\text{m}^2\right) \cdot k_{GA}\left(\frac{\text{mol}}{\text{h}\cdot\text{m}^3\cdot\text{atm}}\right) \cdot P\,(\text{atm})} \tag{A.101}$$

$$\dot{W}_{\text{compressor}}\,(\text{kW}) = \frac{k \cdot R\left(\frac{\text{J}}{\text{K}\cdot\text{kmol}}\right) \cdot T^{\text{gas stream}}_{in}\,(\text{K}) \cdot \dot{m}^{\text{gas stream}}_{in}\left(\frac{\text{kg}}{\text{s}}\right)}{\eta_{\text{compressor}} \cdot (k-1) \cdot MW_{gas}} \cdot \left(\left(\frac{P^{\text{gas stream}}_{in}}{P^{\text{gas stream}}_{out}}\right)^{\frac{k-1}{k}} - 1\right) \tag{A.102}$$

A.2 CAPITAL AND OPERATING EXPENSES

A.3 PROCESSING COST

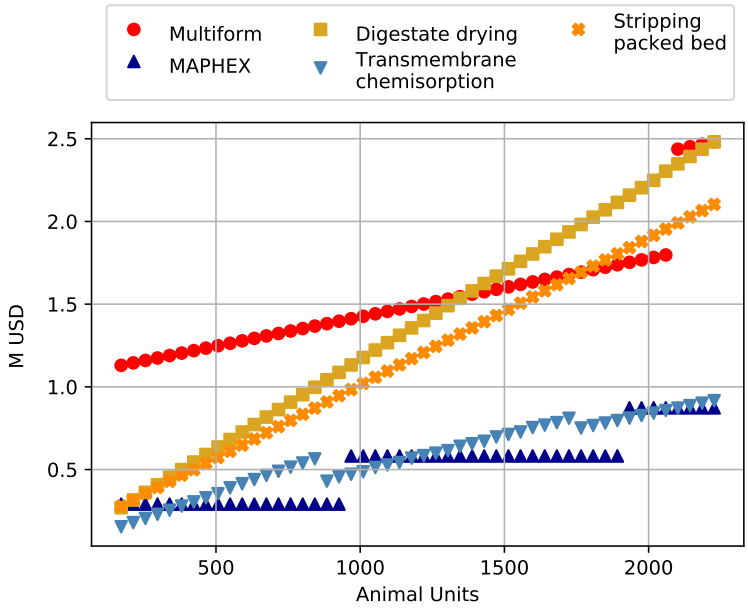

(a) CAPEX

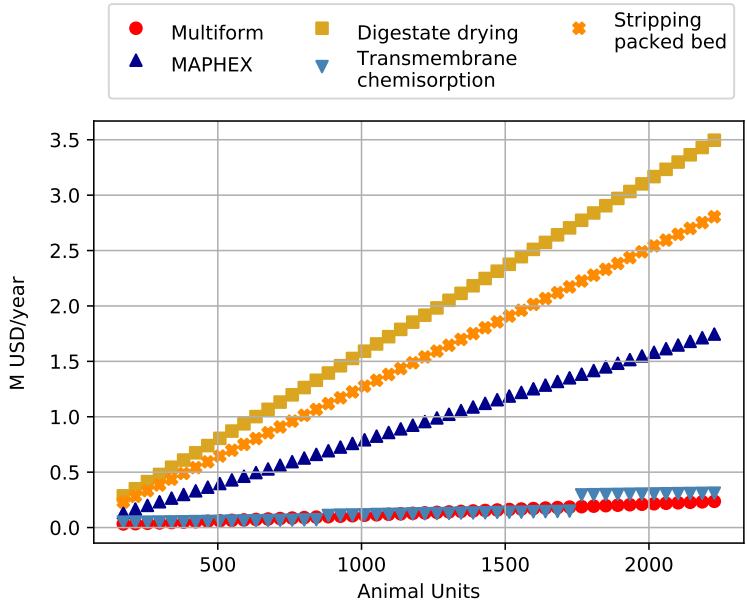

(b) OPEX

Figure A.4: CAPEX and OPEX of the assesed nitrogen recovery technologies, including the cost of anaerobic digestion stage.

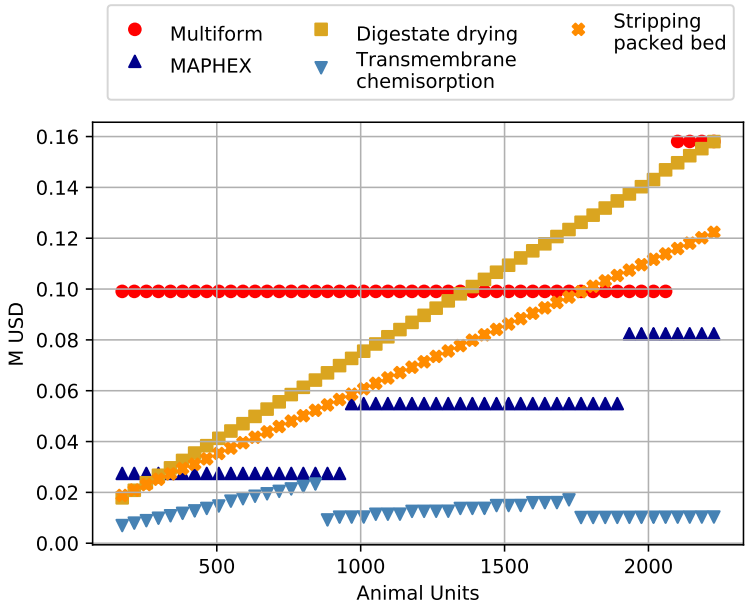

(a) CAPEX

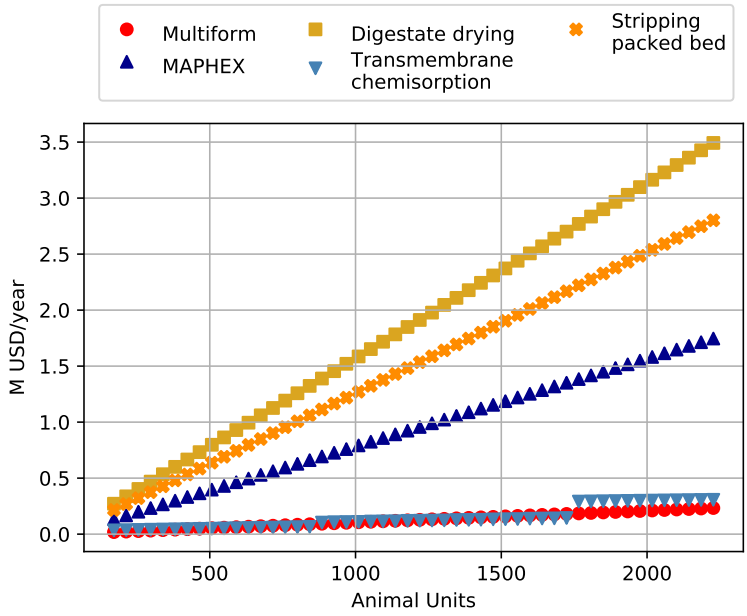

(b) OPEX

Figure A.5: CAPEX and OPEX of the assesed nitrogen recovery technologies, excluding the cost of anaerobic digestion stage.

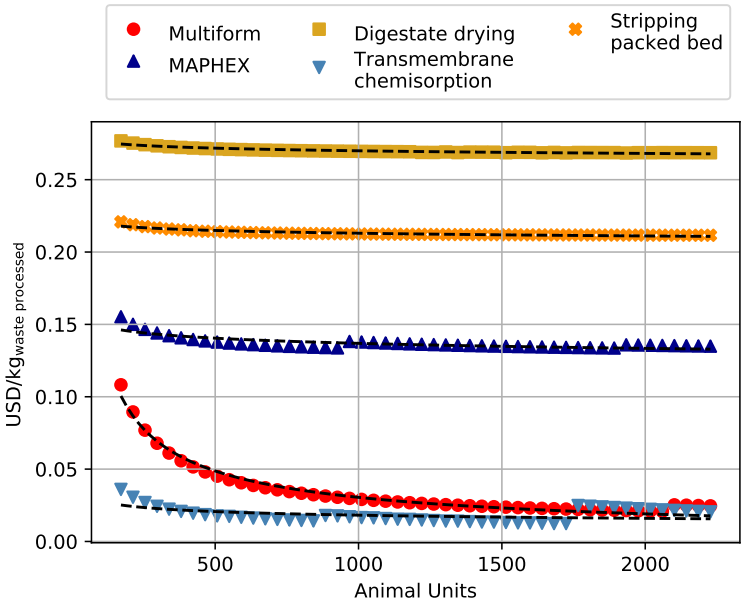

(a) Waste processing cost

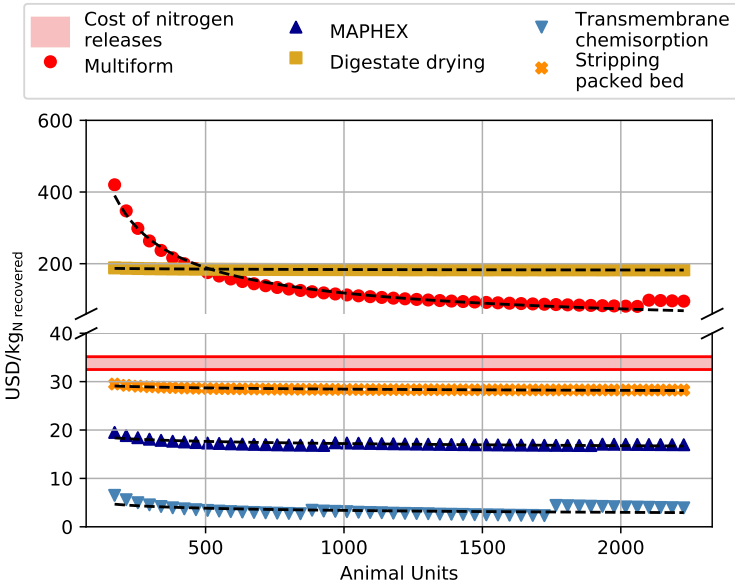

(b) Nitrogen recovery cost

Figure A.6: Processing cost for different livestock facility sizes, excluding the cost of anaerobic digestion stage.

BIBLIOGRAPHY

Agrahari, G. K., Shukla, S. K., Verma, N., & Bhattacharya, P. K. (2012). Model prediction and experimental studies on the removal of dis-

Table A.8: Correlations to estimate the processing cost of the evaluated technologies as a function of animal units (AU), excluding the cost of anaerobic digestion stage.

System	Correlation	Waste processing cost ($\text{USD}/\text{kg}_{\text{waste processed}}$) Parameters	Total nitrogen recovery cost ($\text{USD}/\text{kg}_{\text{N recovered}}$) Parameters
Digestate drying		a=0.289 b=-0.00974	a=196.534 b=-0.00974
Multiform		a=3.261 b=-0.676	a=12660.077 b=-0.676
MAPHEX	$C = a \cdot AU^b$	a=0.177 b=-0.0372	a=22.240 b=-0.0372
Stripping in packed tower		a=0.233 b=-0.0128	a=31.089 b=-0.0128
Membrane		a=0.0410 b=-0.135	a=7.488 b=-0.132

solved NH3 from water applying hollow fiber membrane contactor. *Journal of Membrane Science*, *390*, 164–174.

Bates, R. G. & Pinching, G. (1949). Acid dissociation constant of ammonium ion at 0-50 °C, and the base strength of ammonia. *Journal of Research of the National Bureau of Standards*, *42*, 419–430.

Beddoes, J. C., Bracmort, K. S., Burns, R. T., & Lazarus, W. F. (2007). *An Analysis of Energy Production Costs from Anaerobic Digestion Systems on U.S. Livestock Production Facilities*. US Department of Agriculture (USDA).

Bolzonella, D., Fatone, F., Gottardo, M., & Frison, N. (2018). Nutrients recovery from anaerobic digestate of agro-waste: Techno-economic assessment of full scale applications. *Journal of environmental management*, *216*, 111–119.

Branan, C. R. (Ed.). (2005). *Contents* (Fourth Edition). Burlington: Gulf Professional Publishing. doi:https://doi.org/10.1016/B978-075067856-8/50000-1

Brezonik, P. & Arnold, W. (2011). *Water Chemistry An Introduction to the Chemistry of Natural and Engineered Aquatic Systems*. Oxford University Press.

Church, C. D., Hristov, A. N., Kleinman, P. J., Fishel, S. K., Reiner, M. R., & Bryant, R. B. (2018). Versatility of the MAnure PHosphorus EXtraction (MAPHEX) System in Removing Phosphorus, Odor, Microbes, and Alkalinity from Dairy Manures: A Four-Farm Case Study. *Applied Engineering in Agriculture*, *34*(3), 567–572. doi:10.13031/aea.12632

Couper, J. R., Penney, W. R., Fair, J. R., & Walas, S. M. (2005). *Chemical process equipment: selection and design*. Gulf Professional Publishing.

Fachagentur Nachwachsende Rohstoffe. (2010). *Biogas Guide. From production to use.*

Fowler, B. & Kuroda, S. (1986). Changes in heated and in laser-irradiated human tooth enamel and their probable effects on solubility. *Calcif. Tissue. Int. 38*, 197–208.

Gregory, T., Moreno, E., & Brown, W. (1970). Solubility of $CaHPO_4 \cdot 2H_2O$ in the system $Ca(OH)_2 - H_3PO_4 - H_2O$ at 5, 15, 25 and 37.5 °C. *J. Res. Natl. Bur. Stand. 74*, 461–475.

Hsu, C.-H. & Li, M.-H. (1997). Densities of aqueous blended amines. *Journal of Chemical & Engineering Data*, *42*(3), 502–507.

Larsen, T., Udert, K., & Lienert, J. (2013). *Source separation and decentralization for wastewater management*. Iwa Publishing.

Linstrom, P. J. & Mallard, W. G. (2001). The NIST Chemistry WebBook: A chemical data resource on the internet. *Journal of Chemical & Engineering Data*, *46*(5), 1059–1063.

Martín-Hernández, E., Ruiz-Mercado, G. J., & Martín, M. (2020). Model-driven spatial evaluation of nutrient recovery from livestock leachate for struvite production. *Journal of Environmental Management*, *271*, 110967.

Matches. (2014). Matches' Process Equipment Cost Estimates. https://matche.com/equipcost/Default.html. [Online; accessed 29-March-2018].

Melse, R. W. & Ogink, N. (2005). Air scrubbing techniques for ammonia and odor reduction at livestock operations: Review of on-farm research in the Netherlands. *Transactions of the ASAE*, *48*(6), 2303–2313.

Metcalf & Eddy. (2014). *Wastewater Engineering: Treatment and Resource Recovery*. McGraw-Hill, New York.

Møller, H., Lund, I., & Sommer, S. (2000). Solid-liquid separation of livestock slurry: effciency and cost. *Bioresour. Technol. 74*, 223–229.

Morse, J. W., Arvidson, R. S., & Lüttge, A. (2007). Calcium Carbonate Formation and Dissolution. *Chem. Rev. 107*, 342–381.

Ohlinger, K. N., Young, T., & Schroeder, E. (1998). Predicting struvite formation in digestion. *Wat. Res. 32*(12), 3607–3614.

Penn State Extension. (2016). *Agricultural Anaerobic Digesters: Design and Operation*. Penn State University.

Peters, M. S., Timmerhaus, K. D., West, R. E., et al. (2003). *Plant design and economics for chemical engineers*. McGraw-Hill New York.

PWTech. (2018). *Volute Dewatering Press*. PWTech Process Wastewater Technologies LLC.

Rongwong, W. & Sairiam, S. (2020). A modeling study on the effects of pH and partial wetting on the removal of ammonia nitrogen from wastewater by membrane contactors. *Journal of Environmental Chemical Engineering*, *8*(5), 104240.

Ryckebosch, E., Drouillon, M., & Vervaeren, H. (2011). Techniques for transformation of biogas to biomethane. *Biomass and bioenergy*, *35*(5), 1633–1645.

Seader, J., Seider, W. D., & Lewin, D. R. (2004). *Product and process design principles: synthesis, analysis and evaluation*. Wiley.

Skoog, D., West, D., Holler, F., & Crouch, S. (2014). *Fundamentals of analytical chemistry*. Cengage Learning.

Taylor, A., Frazier, A., & Gurneynium, E. (1963). Solubility products of magnesium ammonium and magnesium potassium phosphates. *Trans. Faraday Soc. 59*, 1580–1584.

Ulbricht, M., Schneider, J., Stasiak, M., & Sengupta, A. (2013). Ammonia recovery from industrial wastewater by TransMembraneChemiSorption. *Chemie Ingenieur Technik*, *85*(8), 1259–1262.

Zhu, Z., Hao, Z., Shen, Z., & Chen, J. (2005). Modified modeling of the effect of pH and viscosity on the mass transfer in hydrophobic hollow fiber membrane contactors. *Journal of Membrane Science*, *250*(1-2), 269–276.